Fatigue Design of Oil Tankers;

A Design Approach

by

Paul Franklin

Dissertation submitted to the Faculty of the

Virginia Polytechnic Institute and State University

in partial fulfillment of the requirements for the degree of

Doctor of Philosophy

in

Aerospace & Ocean Engineering

APPROVED

O. F. Hughes, Chairman

E. Nikolaidis

W. L. Neu

E. R. Johnson

R. H. Plaut

December 1993

FATIGUE DESIGN OF OIL TANKERS;
A DESIGN APPROACH

by

Paul Franklin

Owen F. Hughes, Chairman

Department of Aerospace and Ocean Engineering

(ABSTRACT)

The oil tankers that operate on the Trans-Alaska Pipeline Service (TAPS) route have exhibited a large number of structural fatigue cracks. These cracks can be attributed to the increase in use of high strength steel in tanker construction and to the harsh operating environment in the Gulf of Alaska. In response to the TAPS fatigue problem, this project examines the topic of preliminary design for fatigue resistance. The TAPS tankers have previously been the target of several studies on the subject of fatigue cracking. Most of these studies have concentrated on reducing the costs and risks involved with operating the current tanker fleet. Preliminary design, however, is oriented at reducing the fatigue risk in future tanker designs. To that end, the design method outlined within concentrates on the level of analysis that is appropriate for preliminary design.

The design method consists of four steps: the specification of a wave environment, generation of a hydrodynamic model and subsequent wave loads, evaluation of cyclic stresses and an assessment of fatigue damage. A series of example calculations that is typical of preliminary design has been performed for one of the TAPS tanker classes. These calculations employed Buckley's climatic wave spectra, a 3-dimensional panel based hydrodynamics package by Lin and a Miner's rule fatigue assessment based on the S-N curves of the British Welding Institute.

The example calculations yield two important results. First, relatively inexpensive methods can yield important and accurate fatigue results; for a side shell longitudinal at the water line the example calculations predict a fatigue life of approximately 3 operating years. This corresponds quite well to the published inspection data and obviously represents insufficient fatigue life. Second, local panel pressures can have a significant contribution to, and even dominate, total fatigue damage in the side shell. This contrasts with conventional fatigue studies of ship hulls which focus on global loads; i.e., hull girder bending.

Acknowledgments

In many ways this dissertation does not represent the efforts of any one person. A quick look at the reference list yields many fine engineers and scientists who, either knowingly or not, contributed their efforts. There is, however, both an individual and an organization that deserve special mention. First, my most sincere thanks to Dr. Owen Hughes, my advisor, who not only envisioned this project, but who also contributed immeasurably to its contents. Secondly, I am deeply grateful to the Ship Structures Committee for their generous financial support.

I must also thank all the members of my family for their contribution. Once again though, I have a special commendation for those who went *above-and-beyond*. For their long-term emotional support and encouragement, I thank my parents, Richard and Ann Franklin. And for Lori, who did not hesitate when I mentioned marriage, quitting two good jobs and the life of starving graduate students all in one breath, I reserve my most heartfelt respect.

Table of Contents

Table of Figures

Table of Tables

Chapter 1: Tankers, Fatigue and Design

Introduction

The structural integrity of oil tankers has become an important issue worldwide in terms of both environmental and economic costs. The oil spill in the Gulf of Alaska due to the grounding of the Exxon Valdez and the subsequent public outcry has caused many, including the United States Congress, to re-evaluate the risk associated with oil tanker operations. Even prior to the Exxon Valdez accident, the US Coast Guard, marine operators and various independent experts were investigating the risks involved with structural fatigue of tankers and the means for reducing such risks. This dissertation investigates the most basic form of risk reduction: first principles design of tankers including fatigue resistance.

Steel ships have traditionally been designed for fatigue resistance by means of *rules-based* design. The rules empirically define scantling sizes based primarily on the evolution of ship structural design over many years and the subsequent massive amount of experiential data. Such rules are not well suited to modern ship design where new technologies and subsequent new designs may develop over relatively short time periods. However, the radical changes in technology that often invalidate rules-based design have been mirrored by vast improvements in analysis methods, which should be utilized to minimize the risks associated with new technologies.

The field of marine structures is therefore ready to embark on a new era of design which includes explicit consideration of fatigue damage in realistic operating environments. The transition to full and explicit consideration of fatigue will undoubtedly be a gradual process. The complexity of analysis methods will have to evolve with both the knowledge base of the marine structures community and the power of readily available computing facilities. This dissertation attempts to clarify the current state of affairs in design level fatigue analysis and demonstrates at least one area, panel pressure induced fatigue damage, which has received insufficient attention.

In this introductory chapter a brief synopsis of structural fatigue in modern tankers is presented. The structural loads and other phenomena that cause such fatigue will be discussed as well as possible levels of analysis. The second chapter introduces the general category of tankers termed here TAPS (Trans-Alaska Pipeline Service), and more specifically the Atigun Pass class of tankers which will be used for example calculations. Chapter 3 summarizes some notable efforts in the area of fatigue analysis by other authors, including those procedures and analysis techniques that are incorporated in Chapter 4, which consists of an in-depth look at the proposed analysis method. Example calculations for the Atigun Pass tankers are presented in Chapter 5, and conclusions based on those example calculations are given in Chapter 6.

Tankers and Concern

The issue of oil tanker reliability has taken on new meaning, especially inside the US, with the grounding of the Exxon Valdez. The increased public visibility of tanker operations and the inherent public costs of tanker accidents has left the industry, both operators and regulators, better aware of the importance of reliability. Indeed, the US Congress further

strengthened such awareness in passing the Oil Pollution Act of 1990 (OPA90). OPA90 contains a variety of components including a specification of liability for tanker operators and the forced phase-out of the current oil tanker fleet. However, the OPA90 requirement of double hull ships is only aimed at reducing the dangers associated with grounding and collision. It does not decrease the risk of loss of a tanker's structural integrity due to fatigue. In fact, there is a possibility of increased risk of fatigue failure due to the wholesale redesign of the world's tanker fleet and the increase in exposed structural surface area.

In order to be consistent with the public's demand for safer, spill-resistant ships, the marine community must ensure that all aspects of tanker operations, including fatigue damage, have at least as much safety margin as the new double hulled ships will have with respect to grounding and collision. Unfortunately the Coast Guard report of June 1990 [1] summarized many individual opinions concerning the state of the art in fatigue design with, "Generally, fatigue evaluation is an extremely complex analysis... .Fatigue evaluations are not yet a common and practical component in the design process." Later in this dissertation it is shown that fatigue analysis can vary from the relatively inexpensive (PC based, using pre-existing software tools) to very expensive (supercomputers and the latest research tools). With the undeniable risks involved, it is obvious that some level of fatigue design is necessary, and therefore a clear understanding of all aspects of the origins of fatigue and suitable methods of prediction are needed.

Origins of Fatigue Problems

As mentioned in the Introduction, conventional steel ships have historically not been designed explicitly for fatigue resistance. Instead, implicit fatigue resistance has been

absorbed into rules-based design. Such implicit fatigue design was relatively effective for conventional (small) tankers built of mild steel. The combined introduction of much larger tankers built of higher strength steels has resulted in increased fatigue problems.

The primary fatigue difficulty with higher strength steels is that, in the welded condition, fatigue strength does not increase in proportion to static yield. This is an often misunderstood aspect of fatigue. Higher strength steel is not inherently more susceptible to fatigue. Indeed the fatigue strength of the undisturbed parent metal increases linearly with the yield stress. Rather it is the microscopic geometry of the welded joint, the resulting notch stresses and the residual stresses due to welding that reduce the fatigue resistance of higher strength steel to that of mild steel [2]. Unfortunately, upon the introduction of higher strength steels, safety authorities allowed higher levels of total stress, which meant larger values of cyclic stress as well as static stress. Such higher values of cyclic stress, when multiplied by the stress concentration factors (SCF's) for typical joints, resulted in increased fatigue damage to previously acceptable connection details.

The initial effort to overcome increased fatigue damage has been concentrated on improving the design and construction of connection details in order to reduce the SCF. However, the local cyclic stress at a connection, and thus the resulting fatigue damage, is the product of two quantities: the SCF and the cyclic stress field that is acting in the region of the connection; i.e., the member stress. The stress field (both static and cyclic) is determined by preliminary design, which establishes the scantlings of all of the principal structural members. If the preliminary design does not deal adequately with fatigue the cyclic stress field in the member will be too large, and no amount of detail design will be able to correct for or make up for this inadequacy.

It is not implied here that fatigue cracking will be seen outside of regions of conventional stress concentration. The SCF will indeed always initiate the fatigue crack. Rather, an inadequately sized member will result in fatigue cracks which initiate at even a minimal SCF.

A further aspect of fatigue that is not adequately considered by rules-based design is operating environments. In rules-based design it is difficult to codify the effect that continuous operations in harsh wave environments may or may not have. Later, evidence will be discussed which shows that the TAPS tankers are more prone to fatigue damage than other US vessels. While this may be attributed to faulty design, it is also now known that the wave environment in the Gulf of Alaska is more demanding than is typical. But the environment factor is quite complicated. Mavrakis and Chen [3] have shown that careful consideration is needed in determining the most rigorous fatigue environment; of two wave environments, it is not necessarily the most extreme environment (in terms of wave height) which results in the greatest fatigue damage.

Fatigue Loads

Any structural load with a significant fluctuating component can contribute to fatigue damage. For tankers, significant alternating loads can be grouped into three categories: hull girder bending stress at the wave encounter frequency, hull girder bending stress at the hull's natural frequency, and local panel pressures also at the wave encounter frequency. Such categories are of course artificial because it is the local panel pressures that cause both of the other categories of loading. It is, however, convenient in a historical sense and indeed from a physical understanding to maintain all three categories.

Hull girder bending stress is a quantity derived by considering the ship's hull as a simple beam (girder) which resists bending moments through a linear distribution of longitudinal stress. For a sagging bending moment the stress is compressive at the deck, zero at the neutral axis and tensile in the ship's bottom. For a hogging bending moment the stresses are reversed. Ensuring adequate strength for hull girder bending is an integral part of ship structural design dating back to Brunel in 1852 and the Great Eastern [4]. Thus the calculation of hull girder bending due to a passing wave is part of many ship motion and load programs. Consistent with linear beam theory, the deck and bottom of a ship combine to carry most of the hull girder bending loads, and thus when analyzing maximum load carrying ability, such extreme fiber structures are of primary importance. Indeed, a major fatigue failure of structural members in either the deck or bottom will reduce the ultimate load carrying ability of the hull. As such, the importance of hull girder fatigue due to wave load has been recognized and possibly over emphasized in many works concerning fatigue analysis.

Superimposed over the hull girder response at wave encounter frequency is a response at the lowest natural frequency of the hull girder. This much higher frequency response is generally due to bottom slamming or wave flare impact in the bow of the ship. Recent work with the ARCO tankers by Lacey and Edwards [5] has demonstrated considerable slamming response in tankers. For fatigue, such slamming response is especially crucial because the high frequency can mean numerous cycles accumulate in a relatively short time span. Thus it may be quite important to include the fatigue due to slamming when analyzing structural members either in the ship's bow or members with considerable hull girder stress.

The third category of loads is due to local panel pressure fluctuations. These loads are unique and important because they occur not in the hull girder, but primarily near the mean water line and the ship's neutral axis. Panel pressures are also important because they combine the two worst features of the two categories of hull girder bending. Like the slamming response, the fluctuations of panel pressures contain a larger portion of their energy at higher frequencies then the hull girder response. Unlike slamming, however, panel pressure fluctuations occur consistently throughout the life of the ship and are not restricted to severe seas. Thus the fatigue requirements of ship's side longitudinals are different and not necessarily less intense than those of either the deck or bottom.

Fatigue Analysis

Most of the comprehensive marine fatigue analysis efforts that have either been proposed or implemented are based on some level of spectral analysis. In this case the end product of the spectral analysis is a spectral density function of stress (*vs.* frequency). The statistical properties of this spectrum are then used to calculate the fatigue damage. If linear fatigue damage accumulation and linear stress response to loads are both accepted as sufficiently accurate for fatigue design purposes, there remains one issue whose difficulty dominates fatigue analysis: ship motions and loads in an irregular sea.

There are three reasonably distinct approaches to calculating ship motions and the resulting structural loads due to an irregular seaway: fully non-linear, quasi-linear and linear. The linear analysis method is computationally the most efficient, with quasi-linear considerably more expensive and fully non-linear prohibitively expensive for all except highly funded research endeavors.

When using linear response theory, the response-per-wave-amplitude to any particular frequency wave component in a relatively calm sea is equal to that same frequency of wave component in a stormy sea. Therefore the ship's response to waves needs only be calculated once per operating condition (speed and heading). For head seas and the resulting heave and pitch motions, this analysis is valid up to extreme seas. Unfortunately, a ship's rolling response, and thus also the coupled motions of sway and yaw, is not sufficiently modeled with linear analysis, even in moderate seas. The fully linear analysis method is therefore limited to head and following seas, where roll motions are not significant.

It is often proposed that within any particular sea state, the roll response can be accurately modeled by some equivalent damping factor. Thus the quasi-linear method of fatigue analysis follows the linear method except that separate calculations must now be made for every sea state. For a typical analysis this means more than 12 times as much computational effort (12 sea states plus calculation of the equivalent damping factors).

The fully non-linear analysis also requires a separate analysis for each sea state. In this case the ship is analyzed in an irregular sea, as described by an actual sea state wave spectrum, until the statistical properties of the structural loads stabilize. While there are non-linear codes available that are capable of this modeling endeavor, the author is not aware of any organization which has performed such an analysis. There are therefore no real guidelines as to how much computational expense is involved. It is known from wave data analysis that short-term spectra are statistically stationary on the order of 1 hour, and observations with significantly less duration have insufficient data populations, Hughes [6]. In 1990, Lin [7] reported the performance of LAMP, a fully non-linear code. For approximately 200 body surface panels he achieved throughput on the order of 200 time

steps per CPU hour on a Cray Y-MP single processor supercomputer. For a typical time step of 0.25 seconds and considering extensions and improvements to both the code and computer hardware, it is possible that each sea state calculation could be performed in one or two hours on a supercomputer. This same calculation would have to be repeated for the set of sea states, ship speeds, headings, ballast conditions and wave environments which describe the ship's operating life. A full example calculation for the TAPS tankers would thus require something on the order of 500 CPU hours on the example supercomputer.

Chapter 2: The TAPS Tankers

Introduction

Chapter 1 has briefly introduced the TAPS tankers and their high incidence of structural cracking. Within this chapter a further discussion of the TAPS tankers is presented. This discussion will emphasize the Atigun Pass class on which the author has concentrated his efforts.

General Overview of TAPS Problems

The US Coast Guard, in Report on the Trans-Alaska Pipeline Service (TAPS) Tanker Structural Failure Study [1], brought into the spotlight the mounting concerns of both marine operators and their regulators with regard to structural cracking. The overall concern was effectively summarized in the following quote:

> "... TAPS tankers comprised 13 percent of US flag oceangoing vessels over 10000 gross tons between 1984 and 1988, but accounted for 59 percent of the structural failures... ."

A follow-up report [8] emphasized the fracture history of two specific classes: Atigun Pass and American Sun. For the American Sun class the majority of cracks were found in either the bottom structure or at "rat holes" (small cut-outs) in various unspecified details. For the Atigun Pass class, fractures were described in the deck, the bottom and in side shell longitudinals.

Sucharski and Cheung [9], representing ARCO Marine Inc. (AMI), list nine ships in four additional classes of tankers which AMI uses in the TAPS trade. Although more detailed descriptions of crack types and their distributions were made for only two of these classes, it is stated, "By the mid 1980's extensive fracturing was occurring in many of these ships."

As a result of the Coast Guard reports and related meetings held between the Coast Guard and operators, special inspection programs for tankers involved in the TAPS trade have been developed. Annual inspections of the cargo block following the guidance of a Critical Areas Inspection Plan (CAIP) have been instituted. The CAIP supplies inspectors with detailed information on the fracture histories and repair strategies for individual classes and ships. The scope of impact of structural cracking on the TAPS trade can be quickly summarized; Sucharski and Cheung specify that 100 fracture repairs in a single bi-annual shipyard period is not unusual. Furthermore, additional repairs between scheduled maintenance periods are sometimes required. Obviously, any improvements that could be incorporated in the design and construction of new tankers would provide an economic return.

Atigun Pass Class

Most of the ships and classes operating on the TAPS route have been prone to excessive fatigue cracking. It was noted earlier that the Atigun Pass class was emphasized in US Coast Guard reports. The following discussion describes the ships of this class and the available information on their cracking history.

The Atigun Pass class of tankers consists of 6 single-side, single-bottom ships built by Avondale Shipyards from 1977 to 1979. All are built with a combination of mild and high strength steel. The Exxon Benicia, which is used as an example throughout this study, has

a maximum displacement of 175000 LT. Operating policy typically limits the Exxon ships of this class to approximately 95% of maximum displacement.

The original Coast Guard report [1] limited the discussion to cracking in bilge keels, side shell longitudinals at transverse bulkheads and bottom longitudinals in the vicinity of limber holes. The follow-up report [8] specified cracking not only of side longitudinals 29, 30 and 31 at transverse bulkheads, but also in longitudinals 42,43 and 45 at transverse frames. Bottom longitudinal cracking at the limber holes was also specified. A more detailed description of the side shell longitudinal fractures was prepared for the Benicia's Fall 1991 CAIP. The vertical distribution of side shell longitudinal fractures is shown in Figures 2.1 and 2.2.

The graphic representation of side shell fractures demonstrates some of the earlier concerns and questions pertaining to side shell longitudinal fractures. The most dramatic issue may be the grouping of fractures at the cargo voyage waterline (see especially the starboard or "weather" side), which suggests some mechanism that is most extreme in the splash zone. If a splash zone mechanism were strictly true, an identical peak at the ballast voyage waterline, which does not exist, would be expected. Finally, longitudinals 41 and 44 were significantly less prone to fatigue than those members immediately adjacent.

The most common method of fatigue analysis for ships, that which considers fluctuating axial stresses due to the hull girder bending moment, does not explain any of these phenomena. The waterline is close to the neutral axis, at which axial bending stress is zero. The vast majority of fatigue damage must therefore be due to a different loading phenomenon, most likely local panel pressures.

If local pressures are now considered, the next inconsistency is the reduced amount of fatigue in the longitudinals near the ballast voyage waterline. A first tendency may be to claim that the less heavily loaded ship behaves differently in waves and the result is lower panel pressure loads. While this may be partially true, the most basic reason is the linear sizing, in proportion to hydrostatic head, of the side shell longitudinals. Thus the larger members in the region of L38 (ballast voyage waterline) see smaller alternating stresses than the smaller members near L44 (cargo voyage waterline). This difference in fatigue life, despite identical connection details, tends to strengthen the argument that preliminary design and member sizing are important aspects of fatigue design.

As discussed earlier, there appears to be an anomaly when considering several of the midheight shell longitudinals. Longitudinals 41, 44 and even 46 are within the high risk zone, are sized in terms of the hydrostatic head and indeed have a poor fracture history at transverse bulkheads, but are remarkably free of fractures at other frames. The explanation for this phenomenon is found by comparing the connection detail between longitudinal 44 and a web frame, Figure 2.3, with a typical longitudinal to web frame detail, Figure 2.4, and finally the typical longitudinal to transverse bulkhead detail, Figure 2.5.

Apparently the large brackets used in L41, L44 and L46 (Figure 2.3) reduce the susceptibility of these longitudinals to fatigue. These large brackets have been credited with being both an improved fatigue design detail ("softening" the SCF) and with shortening the effective span (and thus reducing stress levels at the connection). But a more complete and convincing explanation can be obtained by examining the bending moment distribution in a typical side longitudinal segment between transverse frames, which is that of a clamped beam as shown in Figure 2.6. The bending moment and thus

the stress at the end of the bracket, the location most likely to generate a fatigue fracture, is almost exactly zero and this is why little fatigue damage has occurred. In contrast, the smaller brackets used in the details shown in Figures 2.4 and 2.5 have their edges, and thus the SCF, at locations of much higher bending stress. These smaller brackets are therefore much more susceptible to fatigue damage.

Chapter 5 will again consider the TAPS tankers and perform sample calculations to quantify the qualitative arguments presented herein. The qualitative results are enough however, to define the two main points of this dissertation and the recommendations for design contained herein:

1.) Fatigue is just as important during preliminary design, when member scantlings are determined, as during detail design, when connection details are designed.

2.) Local pressures are a critical fatigue load in the side shell.

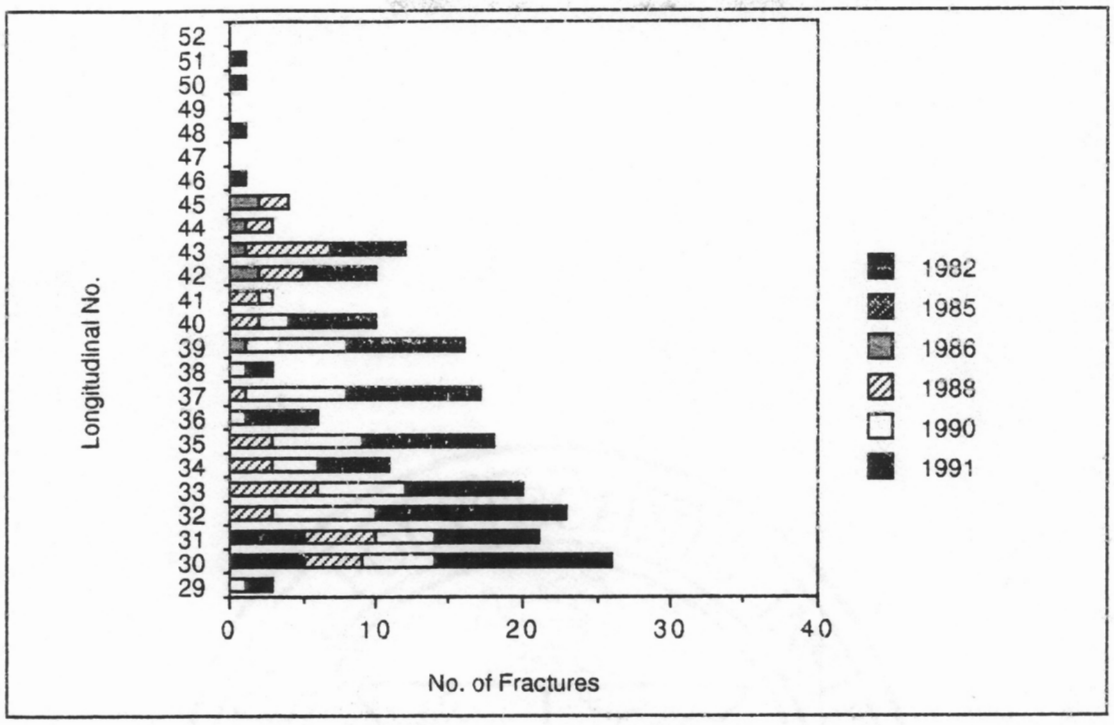

Figure 2.1: Vertical Distribution of Side Shell Cracking, Port Side.

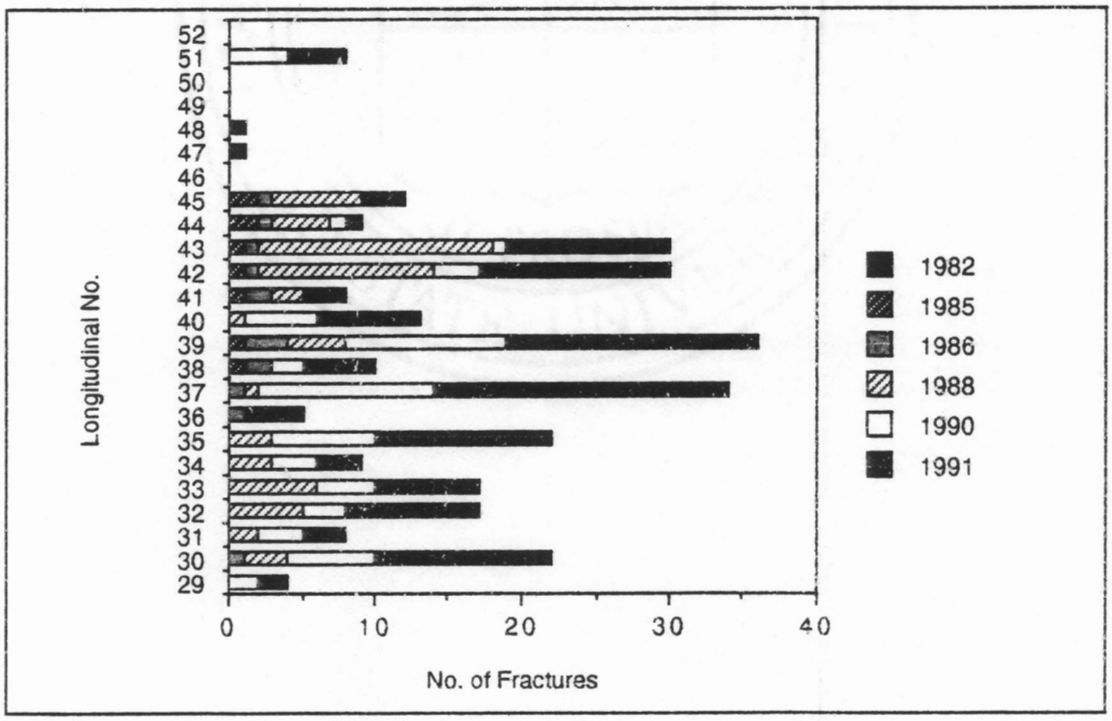

Figure 2.2: Vertical Distribution of Side Shell Cracking, Starboard Side.

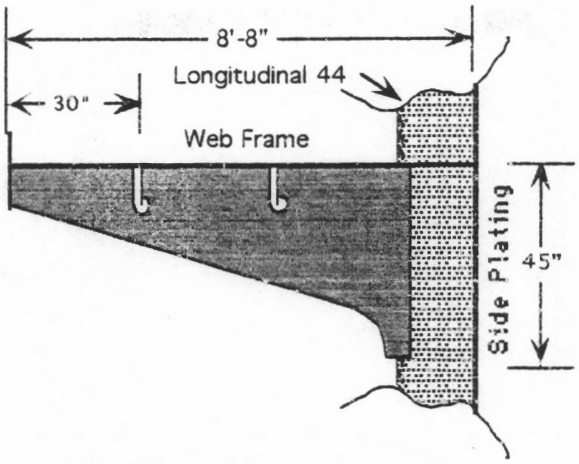

Figure 2.3: Longitudinal 41, 44 and 46 at a Web Frame

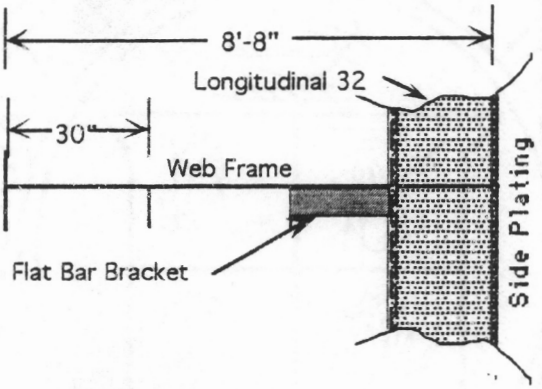

Figure 2.4: Typical Longitudinal at a Web Frame

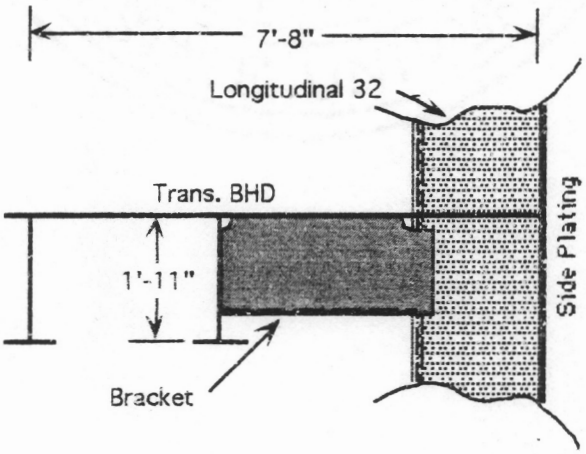

Figure 2.5: Typical Longitudinal at a Transverse Bulkhead

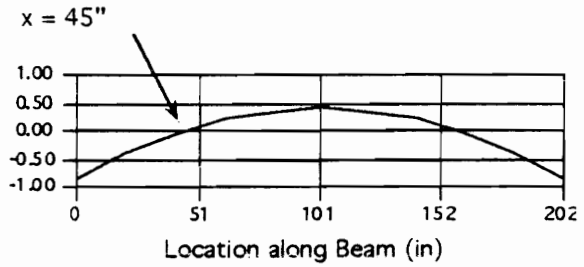

Figure 2.6: Normalized Moment for Clamped Longitudinal between Transverse Frames

Chapter 3: Tanker Fatigue Analysis and Design Methods

Introduction

Fatigue analysis for tankers has recently become a widely considered field. In the proceedings of the Ship Structures Symposium '93 there are six papers considering the subject. In addition, several other authors have published comprehensive works during the time span of this study. The following pages will first discuss the background material and direct contributions made by other investigators to this study. A variety of ship and other marine fatigue efforts will then be presented.

Components of Fatigue Design

Analysis or design for fatigue criteria requires tools from at least four disciplines from within the greater field of naval architecture. The author has drawn on recent advances in several of these fields for improved analysis tools. Chief among these improved tools are the hydrodynamic routine SAMP by Woei-Min Lin and the parametric wave descriptions of the TAPS tanker route by William Buckley.

Invariably, fatigue analysis methods assume that a random sea, and ship motions in such a sea, can be decomposed into the linear sum of many regular waves. This linearity of the ship/wave system was originally proposed by St. Denis and Pierson [10] and has since become widely accepted within the industry. Only quite recently has the importance of a nonlinear ship/sea system been emphasized, see for instance Buckley [11], and nonlinear

analysis tools have begun to appear (e.g., Large Amplitude Motion Program, a nonlinear version of the SAMP computer code). Nevertheless, the great majority of a ship's life, and thus the accumulation of fatigue damage, is spent in non-storm conditions.

Wave Definition

In structural design, one of the first, and often least understood, engineering requirements is an adequate definition of the loads. While so-called dead loads (permanent loads associated with the structure and its contents) are relatively easily established, structural live loads are frequently less well known. A designer must establish both the loads that are present in day-to-day operations and those which threaten the safety of the structure and its occupants under extreme conditions. Often these live loads are influenced not only by the intended use of the structure, but also by the surrounding environment.

In many structures, including buildings and bridges as well as ships, two distinct types of live load must be accounted for: every-day operating loads and long term extreme loads. It is relatively obvious that controlling stresses due to static floor loads in an office building is a separate problem from ensuring sufficient energy absorbing ductility during a major earthquake. In contrast, it may be less obvious that, in addition to ultimate ship strength in an extreme storm, another design concern is high cycle fatigue due to the constant wave and motion induced pulsating pressures on a hull.

Because of their inherent mobility, ships present additional difficulties concerning load definition. Whereas the designer of a land-based structure knows exactly the location for which the structure is destined, and thus has a good idea of the risks associated with earthquake, wind and other environmental loads, the marine designer is likely to have little more than a designation of coastal or offshore. Thus the generic designation often applied

is *worldwide unlimited service*, with a design wave environment based on the North Atlantic.

The practice of designing ships to withstand the rigors of a fixed and specific extreme environment is soundly based and has the advantage of offering ship owners and operators assurance that their ships are built to withstand such rigors when necessary. However, it has been shown (see for example Mavrakis and Chen [3]) that for two long-term wave environments, the environment which is apparently most severe in terms of ultimate loading is not necessarily most severe in terms of fatigue. Improvements in computational abilities have made it possible to demonstrate that a ship is not only adequate for a simplified design environment, but is also adequate for its intended, or most likely, operating environment.

For the TAPS tankers on which this study focuses, very accurate environmental data are available through the long-term wave height spectra observed by NOAA wave buoys and the work done by William Buckley. He examined a large body of wave spectra and subdivided regions of the oceans into wave climates for which characteristic values of modal period τ_p and wave length λ can be identified [11]. Specifically, for the TAPS tanker route there are two distinct wave climates: Northern High Latitude and West Coast Long Period. Buckley averaged the individual wave spectra within 1 meter significant wave height intervals to define a single Climatic Wave Spectrum (CWS) for each wave height class and wave climate. In order to simplify the structural calculations these CWS are represented using Ochi 3 parameter spectra. The percentage of occurrence of each wave height class was also determined for each buoy location. Finally, the directionality of the wave spectra was equated to the recorded wind direction.

The objective data obtained from the NOAA wave buoys and the consistent analysis performed by Buckley have resulted in wave data free from many of the uncertainties evident in other wave environment descriptions. For worldwide coverage, the Marsden Square data by Hogben and Lumb [12] are frequently used. Hogben and Lumb based their work on voluntary reporting of observational data by merchant ships. A slightly more objective set of wave data, covering only the North Atlantic, was developed by Walden [13]. He used observational data from trained observers on fixed location weather ships.

The US Navy's hindcast program is an alternative approach to either wave buoy or observational data. In this program the Navy used observed wind data to hindcast sea conditions throughout the northern hemisphere for a specific 20 year period. Portions of the hindcast data have been presented in suitable form for design analysis by Cummins and Bales [14].

The tradeoff between all wave environment descriptions is accuracy *vs.* coverage. Very good data, including directional information, are available in the limited ocean areas for which there is wave buoy coverage. More extensive coverage of the entire Northern Hemisphere is available, but there are uncertainties in the hindcast process. Finally, world-wide coverage is possible, but only given the rather large uncertainties of observational data.

Hydrodynamics

Any truly analytical approach to fatigue design or analysis depends on accurate calculation of dynamic loads due to ship motions in waves. Such an analytical approach is necessary because it avoids the enormous time and expense entailed in modeling and wave tank

studies. The most common method used to perform this analysis is strip theory, and the US Navy's widely used Ship Motions Program (Meyers, [15]) will be utilized in some of the example problems discussed herein. However, larger emphasis will be placed on the linear 3-dimensional potential flow program SAMP (Small Amplitude Motions Program).

Strip theory reduces the hydrodynamics of 3-dimensional flow past the hull to a 2-dimensional flow past a series of independent prismatic bluff bodies, roughly akin to cylindrical flow. Each bluff body has a cross section which is representative of a region of the hull, and thus the hull is replaced by a series of prismatic segments commonly referred to as "strips". The simplification of the hull in this manner eliminates the interaction of the ship's forward speed with the hull's lengthwise variation and thus results in a relatively inexpensive computation for each strip. After solving such a 2-dimensional flow problem over each independent strip, the individual solutions are combined to calculate the total hydrodynamic force acting on the ship. Such calculations have long been considered sufficient, especially for overall integrated quantities, but strip theory does not directly provide accurate values for the local pressures acting on structure.

In order to improve the accuracy of the hydrodynamic calculations for the case of a ship with constant forward speed and in order to obtain localized panel pressures, SAMP has been employed on this project. Woei-Min Lin of Science Applications International Corporation (SAIC) has developed this fully 3-dimensional linear hydrodynamics package. SAMP's basic methodology is summarized concisely in the user's manual [16]:

> SAMP calculates the hydrodynamic forces assuming potential flow, and satisfies a linear free-surface boundary condition on the mean position of the free surface. ...In the SAMP calculation, the body boundary condition is satisfied at the mean position of the moving body. The incoming wave can take any form. The solution is found in the time domain and so simulates general unsteady motion.. The hydrodynamic problem at each time step is

solved with a potential formulation, modeled by a three-dimensional transient Green Function.

SAIC is currently in the process of adding semi-empirical viscous forces to those computed through the basic potential flow calculations. Such viscous forces become significant for rolling motions (about the ship's longitudinal axis) when the ship is at an oblique heading to the predominant seaway. Viscous forces are implemented through similar methods as those used in the Ship Motions Program. Such an approach has the advantage of being both computationally inexpensive and quite well established.

Structural Analysis

Marine structural designers need to consider fatigue not in isolation, but in conjunction with many other structural concerns. It is therefore one of the aims of the current project to develop a fatigue analysis method that can be incorporated into the MAESTRO structural design program. MAESTRO enables the designer to rapidly develop whole ship structural models and to calculate stresses by finite element analysis. MAESTRO then computes the failure stresses and other limit values for over 30 modes of failure and compares the actual values to the corresponding limit values. At this point it is the designer's choice whether or not to continue the analysis and have MAESTRO adjust scantling (member) sizes to optimally satisfy all limit states.

Incorporating fatigue analysis into the MAESTRO program will result in an additional, rather complex, limit state. As a practical measure it will probably be best to use this limit state as a go, no-go criterion.

At the present time the fatigue limit state calculation is not performed internally to MAESTRO. Rather, MAESTRO can be interfaced with SAMP to produce stress

information. The stress values are then processed externally using the principles discussed in the following section.

Fatigue Assessment

Design level fatigue assessment in marine structures is dominated by methods that include S-N curves and the linear accumulation of fatigue damage proposed by Palmgren [17] and Miner [18]. The S-N curve is a linear plot of log S *vs.* log N, where S is the range (double amplitude) of alternating stresses, and N is the number of cycles to failure at a constant value of the stress range, S. The British Welding Institute has published a widely used set of S-N curves [19] based on the work by Gurney [20]. In applying the S-N curves and Miner's rule, the derivation by Rice [21] of the statistical distribution of amplitude peaks (Rayleigh) for a narrow banded, stationary, Gaussian process is often incorporated. The result is an explicit formula for fatigue life in terms of the S-N parameters and the spectral moments of the stress distribution.

Several adjustments must be made to the derivation in order to calculate lifetime fatigue damage. Most importantly, the sea surface elevation is neither strictly narrow banded nor is it statistically stationary in the long term. The latter difficulty is reconciled through the use of full spectral analysis. In fatigue terms, a full spectral analysis involves subdividing the ship's life into a number of segments (each of which is stationary), computing the fatigue damage during each segment and summing the fatigue damage across segments to compute the lifetime damage. For ships these segments are defined by each combination of ship speed, sea state, relative wave heading and draft (Wirsching [22], Chen and Mavrakis [3]). An empirical adjustment , called a rainflow correction factor, for the bandwidth of each of these short term processes has been developed by Wirsching and

Light [23]. This adjustment factor simulates the stress range counting results of the rainflow technique by modifying the narrow band result.

Accepting both an S-N approach and the Palmgren-Miner linear damage accumulation rule is, at this time, a necessary step in performing whole ship fatigue analysis. Important real-life features of fatigue are omitted by such restrictions. The omissions or simplifications include important phenomena such as the differentiation of crack growth *vs.* crack initiation, as well as the importance of the chronology of the load history. The existence and possible detrimental effect of mean stress on the fatigue life is also omitted in the particular derivation used here. Such an approach has been used widely throughout the industry and is included in many of the other fatigue analyses discussed later in this chapter. The neglect of mean stresses was shown by Wirsching and Light to be of little consequence for high-cycle fatigue (when alternating stress is small compared to elastic yield stress).

A final issue that appears in the fatigue assessment, is in regard to the multiple stress causing mechanisms present in a ship's hull. Although essentially all loads on a ship are the result of the seaway, a single seaway can have multiple load effects. Much of the results section of this study will concentrate on comparing fatigue due to overall ship response (hull girder) and fatigue due to local response. While both responses will be calculated simultaneously from the same set of uniform waves, the resulting statistics will be quite different. Figures 3.1 and 3.2 portray how the overall response of a ship filters out short period waves when considering hull girder bending, but no such attenuation is present for local panel response. Indeed, because of the rapid fluctuation of panel stresses, the total accumulation of damage in the panel case is increased for short period waves.

The fatigue damage caused by simultaneous, but independent load mechanisms is a intriguing problem. If the two mechanisms have very similar frequency contents, the narrow-banded assumptions used in most simplified fatigue assessments will remain valid. If the frequency content of the mechanisms is markedly different, the narrow banded assumption will be violated and more sophisticated means of counting stress cycles may be required. Even more difficult than counting the stress cycles and their magnitude, is generating the actual stress history. Careful tracking is required of not only the stress amplitude with respect to frequency, but also of the phase of the cyclic stress *vs.* the load.

This dissertation does not attempt to resolve the issue of simultaneous loads and the effect of their interaction on the total fatigue damage. The total damage is assumed to be simply the sum of the damage caused by the two independent phenomena. This stance is somewhat justified by the results of Chapter 5; these results show that for large regions of the ship, only one load mechanism dominates the fatigue damage. The dominant mechanism changes from region to region, but, again, within each region one load dominates fatigue.

Other Efforts in Marine Fatigue

As discussed in the introduction to this chapter, numerous research groups in both the commercial and academic arenas have worked on the subject of marine fatigue. This work varies from fairly early examples of explicit fatigue analysis by researchers at the David Taylor Research Center to recent extensive fatigue calculations performed by marine operators. The following is a brief literature review of important fatigue analysis efforts with an emphasis placed on those publications which were available as input to this investigation.

David Taylor Research Center

Approximately a decade ago Sikora, Dinsenbacher and Beach outlined a procedure in use at DTRC for performing fatigue analysis of ships [24]. Their paper uses experimentally and empirically derived response amplitude operators (RAO) to relate hull girder bending moment to unit amplitude waves. The RAO's are then multiplied by known wave spectra to compute a series of bending moment response spectra and their respective probability density functions. From the probability density functions, a histogram of cyclic stress amplitude *vs.* the number of cycles for which the stress value is exceeded was created. Sikora et al. then demonstrated how to directly apply the Palmgren-Miner cumulative fatigue damage theory to the histogram, termed a lifetime fatigue spectrum, in order to compute fatigue life.

The fatigue analysis presented here therefore differs from the Sikora et al. approach in four significant areas. First of all, physical modeling and extensive tank testing of the ship is not required. Secondly, the analysis is not limited to overall ship quantities such as hull girder bending. Thirdly, several well-known statistical procedures can be implemented to streamline and improve the fatigue damage calculation. Finally, a specific set of widely available S-N curves is incorporated.

American Petroleum Institute

A second existing source of guidance for analyzing fatigue in ocean structures is the American Petroleum Institute (API), which devotes a chapter in its RP-2A [25] to fatigue analysis. The API RP-2A outlines a basic fatigue method for offshore structures. The technique includes recommendations for the wave climate description, dynamic modeling of the structure, development of the stress transfer function and calculation of the fatigue

damage ratio. The API recommendations are limited in generality; they consider only open-framed platforms consisting of tubular members. The recommendations are also limited in scope; [25] is a publication of recommended practices and does not specify analysis procedures in detail. The research directed by Wirsching [22,23] in support of the API guidelines contains specific recommendations in terms of the use of S-N curves and spectral fatigue analysis methods.

Structural Maintenance Project

Very recently a Joint Industry Project titled the Structural Maintenance Project, or SMP, based at the University of California at Berkeley, published a series of volumes entitled *Structural Maintenance for New and Existing Ships* [26]. The Berkeley SMP, as the name implies, is a broad based study on structural maintenance of existing ships. Issues addressed in the study include corrosion, fatigue, structural monitoring and repair management. Their fatigue analysis method therefore differs from those previously mentioned in that it is mainly intended for the analysis of existing ships rather than design of new ships.

Because of the orientation of the SMP towards ship maintenance, the method and the results presented herein are distinct from and quite complementary to those of the SMP. The most significant differences between the two projects are:

1.) SMP uses less precise wave data, based on Marsden squares rather than local and precise climatic data (from wave buoys).

2.) For hydrodynamic analysis, SMP uses strip theory instead of a 3-D panel method.

3.) SMP uses local FE analysis of specific joints and corresponding hotspot stresses in the fatigue analysis, in conjunction with either hotspot S-N curves

or fracture mechanics for failure criteria. In contrast, our method uses the aforementioned joint classification system and S-N curves.

The first difference is primarily an issue of availability. The improved wave data from NOAA buoys and the work Buckley has done to convert the raw data into a usable engineering format are quite recent and are not yet widely available. Even when published, Buckley's data will be limited to those ocean areas for which NOAA buoy data exist (primarily North American coastal waters). Unfortunately, the wave directionality for the published Marsden squares data is not sufficiently differentiated by wave height to be an accurate basis for calculations.

The second difference may also be considered an issue of availability. Efficient 3-D panel based hydrodynamic programs, while certainly a large improvement over strip methods, are relatively new.

The use of local FE analysis on specific joints is an important step in analyzing existing structures, especially when concerns of continued crack growth arise. However, such a process is computationally quite intense and is, as of yet, still too cumbersome for design techniques.

Failure criteria consisting of hotspot S-N curves or fracture mechanics are also appropriate for analyzing existing problematic structures, but have drawbacks in terms of a design method. One of the largest difficulties with hotspot S-N curves is that no widely accepted collection appears to exist. Even SMP conceded as much when they took non-hotspot curves and scaled them according to engineering judgment. As for fracture mechanics, this is again a rather complicated analysis best suited for examining known problem areas.

American Bureau of Shipping

The American Bureau of Shipping (ABS) has developed and published the design document Guide for the Fatigue Strength Assessment of Tankers [27]. In this document ABS sets forth a simplified method for fatigue assessment. The Guide implicitly includes the same basic elements as the fatigue analysis methods described above; the scope of these implicit elements is summarized in the guide's preface:"... considered in the derivation of the criteria are: the Palmgren-Miner linear damage model, S-N curve methodologies, a long term sea environment representative of the North Atlantic (which is to be considered for unrestricted service classification), and a nominal vessel service life of 20 years." However, because the derivation in the Guide simplifies, condenses and combines these elements, it also limits the fatigue assessment in terms of both accuracy and flexibility. The guide addresses this concern and recommends that more elaborate analysis methods be required in cases where the applicability of the derivation is in question.

In September of 1993 ABS began to market its new tanker design software, SafeHull. This program is to be used both for the design of the midbody portion of tankers, and also for classification (approval) purposes. SafeHull internally incorporates some aspects of the Guide. With ABS incorporating the dual responsibilities of design and approval within a single software package, there is substantial need for efficient and rapid means of independent confirmation.

ARCO Marine

Sucharski and Cheung [9] have published the results of an extensive fatigue analysis of the ARCO operated TAPS tankers. Their effort included an alternative presentation of the

NOAA wave buoy data by Ocean Systems Inc., which broke the sea spectra into monthly categories as well as geographic categories. Their work also included fine mesh modeling of several critical and fatigue prone details. One of the most distinctive results for this project was the comparison of fatigue damage vs. weather conditions (winter months were up to 10 times as damaging as the summer months). Also significant was their ability to quite regularly predict fatigue life in several connection details and the effect this had on repair plans. Although data are presented which indicate that mid-height shell longitudinals are subject to fatigue fracture in the ARCO operated TAPS tankers, Sucharski and Cheung did not report any results considering the effect of dynamic pressures on the side shell.

SSC-367 Comprehensive Marine Fatigue Summary

Capanoglu [28] has published a comprehensive overview of marine related fatigue analysis issues in SSC-367, *Fatigue Technology Assessment and Strategies for Fatigue Avoidance in Marine Structures*. Although this document was published too recently to be of substantial use to the current project, it includes an excellent overview of marine fatigue issues and a comprehensive list of 125 publications. Capanoglu's work would be an excellent starting point for any study on marine fatigue assessment.

Figure 3.1: Tanker in Short Period Wave

Note: High frequency, short period waves create buoyancy at many intermediate points along the hull. The alternating bending moment for such waves is effectively attenuated. Panel pressures, however, respond to the individual wave crests and are not attenuated.

Figure 3.2: Tanker in Long Period Wave

Note: Low frequency, long period waves concentrate bouyancy forces at one or two points along the hull and tend to cause maximum alternating bending moments.

Chapter 4: A Fatigue Design/Analysis Method

Introduction

Whereas the previous chapter followed the historical development of fatigue analysis in general and more specifically the methods the author has chosen to apply, this chapter is intended as a step-by-step guide which describes an effective fatigue analysis. The chapter is arranged under four headings (which are familiar from the prior chapter): wave environment, hydrodynamic analysis, structural analysis and fatigue assessment. As noted in the previous chapters, the procedures below are not unique to this project or even to the field of ship structures. However, the specific combination of procedures, consideration of multiple load types and general application is in itself significant.

Again, the overall design/analysis procedure can be considered as a four step process. First, the wave environment for the operating life of the vessel must be succinctly specified. Second, hydrodynamic analysis must be performed to generate a frequency based transfer function between wave height and the load quantities of interest (hull girder bending moment and panel pressures). This must occur for each wave heading and operating condition. Thirdly, a structural analysis must be performed to generate a transfer function between load and member stress. The previously determined wave spectra are then multiplied by both the unit wave and unit load transfer functions to establish the response spectra. Finally, in the fourth step, the spectral moments of the response are computed and the incremental damage ratio is found.

Wave Environment

A spectral wave description for the operating lifetime of the ship is required for this analysis. In general, any reliable wave data with the following characteristics could be implemented:

1.) Segmented into multiple wave-height sea states (≈10)

2.) Known percentage-of-occurrence for both sea state and direction

3.) Concise parameter based summary of spectra (not necessary, but improves computational efficiency)

4.) Representative of ship life (calculations should be performed for every distinct environment)

From the criteria above, any conventional wave scatter diagram, whether generated through a hindcast model, observations, or measurements could be employed. In the case of the TAPS tankers (and other ships operating in the waters surrounding North America), Buckley's wave spectra, as derived from NOAA wave buoy data, are a highly accurate source.

Buckley's spectra for the TAPS route have been included as Appendix A. Four buoy locations (with percentage of occurrence data), spanning the two climatic wave spectra that Buckley has specified for the region, are given. Each buoy location is further delineated into 13 sea states and 8 ship headings. The spectra themselves are specified using Ochi's 3-parameter method. The equation for Ochi's 3-parameter wave spectrum is

$$Sw(f) = H_{m_0}^2 \; Amp\left(\frac{f_{pr}}{f}\right)^{4\lambda} \frac{1}{f} \exp\left(-(\lambda + 0.25)\left(\frac{f_{pr}}{f}\right)^4\right)$$

where: H_{m_0} is the significant wave height

f is the frequency

f_{pr} is a characteristic modal frequency of generalized CWS

λ is a nondimensional shape parameter for Ochi 3P wave spectrum

Amp is a nondimensional amplitude factor

The wave frequency spectrum is based on a data collected by a fixed observer, the wave buoy. A ship experiences a slightly different spectrum due to its forward speed and relative heading to the wave. The excitation frequency the ship experiences is called the encounter frequency, f_e, and is given by,

$$f_e = f_w\left(1 - 2f_w\pi\frac{V_{ship}}{g}\cos(\theta)\right)$$

where: f_e is the encounter frequency

f_w is the fixed observer wave frequency

V_{ship} is the forward speed of the ship

θ is the relative heading of the ship with respect to the wave

g is the acceleration due to gravity

The area under the wave spectrum curve is a measure of the energy content of the sea. Because this energy content must be independent of the observers reference frame (fixed or ship-based), the amplitude of the wave spectra must also be adjusted.

$$S(f_e) = \frac{S(f_w)}{1 - 4f_w\pi\frac{V_{ship}}{g}\cos(\theta)}$$

Hydrodynamics

The end results of the hydrodynamic analysis are frequency based transfer functions between unit wave height and structural loads. Such transfer functions are independent of the wave spectra, but are dependent on relative wave heading, ship draft and speed. For the analysis of a TAPS tanker there are 8 headings, 2 drafts and 1 ship speed. Sixteen

transfer functions are thus required for each structural load. Fortunately the transfer functions for all structural loads can be computed simultaneously by SAMP.

The SAMP user manual, Lin and Meinhold [16], and several papers by Lin [7] discuss the use of the SAMP program in general. This section does not intend to replace those references, but instead discusses some of the more significant steps and procedures required for performing a SAMP analysis. The issues to be discussed herein include: generation of a geometric model, required frequency band, choice of sea type, and several specific modeling parameters.

The initial stage of the hydrodynamic analysis entails creating a geometric model. This model is a panel based description of the ship's hull below the mean waterline. Many in the ship structures community would find it most convenient to generate such a model within the program FastShip by Design Systems. The FastShip model can then be modified by a standard panel manipulations program or used directly after transformation by a simple FORTRAN program. It is also quite possible to manually generate the model from a set of line plans and a table of offsets. Independent of how the model is generated, it should consist of a half hull of 150 to 250 panels. In generating the panel model, consideration should only be made to the surface geometry and the hydrodynamic calculation; the hull structural geometry is not important at this time. Indeed SAMP will, at the user's request, redistribute the panels based on its own requirements. Panels should have width to height ratios on the order of 1. The user must also avoid panels intersecting the waterline at shallow angles; such panels introduce large numerical errors and even instabilities in the computation. Once a suitable geometric model is created, work on the actual hydrodynamic analysis is possible.

One of the first issues to arise in computing the frequency based transfer function is the frequency range which must be considered, The first and most obvious cut-off is the frequency content of the wave environment. If the effective energy content at a particular frequency is nearly zero, then the transfer function at that frequency is not necessary. For the TAPS data provided in Appendix A, significant wave energy occurs in the frequency band of 0.05 to 0.3 Hz (with the availability of excess computing power, a more conservative band would be 0.03 to 0.5 Hz). If calculations strictly for bending moment are being made, the upper cut-off can be reduced substantially. The reduction is possible because the integration of many high-frequency/short-period waves tends towards zero for over-all hull girder quantities (see again Figure 3.1). An intuitive guideline for such a limit is

$$\lambda_{wave} = \frac{L_{ship}}{10} \qquad (4.1)$$

where: λ_{wave} is the length of a single wave

L_{ship} is the waterline length of the ship

In the case of the TAPS tankers this would reduce the upper band limit to approximately 0.25 Hz. If a more general fatigue analysis is performed, there is no advantage to such a reduction; relatively high frequency waves are important to local structural fatigue and the bending moment for the high frequency waves is available for little extra cost.

Further discussion of the hydrodynamic analysis is predicated by SAMP being a time-domain calculation. There are thus two manners in which to proceed. The most intuitive fashion may be to perform a separate analysis for several regular waves and interpolate the frequency transfer function from these points. Possibly a more efficient and more comprehensive method is to use a random wave made up of components from the same

frequency band as the desired transfer function. The resulting response history can then be analyzed by Fourier methods to yield the required transfer function. The author has chosen the first method because of its simple and direct nature. In future efforts the second method should be implemented due to its potential for computational savings. When using discrete waves, judgment must be applied for determining the number of frequency points calculated. The analysis uses 10 points as a standard basis; the figure is reduced or increased depending on the smoothness of the process.

Several of the modeling parameters for SAMP must be modified to reflect the frequency of the incoming wave, the ship's forward speed and the ship's heading. The first parameter to consider is the time step. Lin specifies that 30 time steps per incident wave are "more than adequate"[7]. A parameter heavily affected by the time step size is the memory length. SAMP calculates the effects of hull generated waves for a specified number of time steps after they are generated. Lin suggests that the memory effect should be at least as long as it takes the ship to move one ship length. Therefore to analyze an 850 foot ship moving at 15 knots into a 0.05 Hz wave requires a time step of 0.67 sec and a memory effect of 51 steps (34 sec/0.67 sec). The same ship heading into a 0.25 Hz wave requires a time step of 0.13 sec and a memory effect of 255 steps. The hydrodynamic calculation is dominated by the effort required to compute the memory effect; computation time will be approximately five times longer for the high frequency wave, and temporary disk storage of approximately 100 Mb is required.

A final parameter driving the cost of the SAMP calculations is the total number of time steps required. The SAMP calculation effectively starts with the ship at rest and abruptly imposes a wave field. This is quite different from a ship in a realistic narrow banded sea, where the amplitude and frequency of the incoming wave content tends to vary slowly in

time. The sudden imposition of the wave forces will cause transient motions and loads at the natural frequencies of the buoyant system. The SAMP analysis must be performed for enough total time steps for these transient motions to damp out. For low frequency waves this may take as many as 4 or 5 wave crests. Thus again for a 0.05 Hz wave, the first 80 seconds or 120 time steps is discarded because of transient motions. The total analysis for the 0.05 Hz wave then consists of 240 time steps of 0.67 seconds each and a memory effect of 50 steps. On a 486 based PC the calculation would take approximately 3 hours. For the 0.25 Hz wave, transient motions are insignificant. The analysis requires 300 time steps of 0.13 seconds and a memory effect of 255 steps. On the same 486 PC the computation time is increased to approximately 14 hours.

After completion of enough SAMP runs to sufficiently describe the frequency range of interest, the final stage of the hydrodynamic analysis is to develop the frequency domain transfer functions (FTF) between wave height and load. The SAMP program itself generates a time history, for each wave run, of vertical bending moment at any desired cross section. It is a simple matter to then extract the response amplitude at a wave frequency either directly from the time history or by transforming the time history to the frequency domain and examining the response peak (the response peak should occur at wave encounter frequency).

Calculation of the panel pressure FTF is slightly less direct. SAMP does not record total pressures; instead, a time history of the location and orientation of the ship's center of gravity is stored along with the perturbation pressure for each panel. Such perturbation pressures are the pressures caused by the presence of the hull in the otherwise undisturbed wave. For the linear theory of ship motions, two other pressures are present: the hydrostatic pressure due to the panel control point's instantaneous depth beneath the mean

water surface, and the Froude-Krylov pressure or the internal pressure of the undisturbed wave due to particle motions. The second two components of pressure, which are included in SAMP's equations of motion, but are subsequently discarded, are recomputed by a post processor to SAMP and added to the first component to generate a time history of panel pressures at any requested point.

The post processor interpolates pressures for any point on the hull below the mean waterline. This interpolation process allows the panels used in the hydrodynamic model and those of the structural model to be essentially independent; no one-to-one correspondence of panels is needed, but only an over-all equivalence of the underwater geometry.

There are two readily identifiable problems with the hydrodynamic analysis just described. First, the widely recognized non-linear roll damping, which affects not only roll, but also the coupled motions of sway and yaw, is not included. Secondly, the high frequency wave analysis is excessively expensive; there are little or no ship motions in response to the high frequency waves, and therefore much of the computational effort of a ship motions package is unnecessary. In the analysis to follow, an attempt will be made to address both issues with a single solution.

SAMP is based on potential flow theory. The forces arising from potential flow dominate motion in at least three degrees of freedom: surge, heave and pitch. For roll, and the coupled motions of sway and yaw, viscous forces become important. Although SAMP will in the future have the capability of using semi-empirical formulae to calculate viscous effects, the current version does not. The US Navy's Ship Motions Program (SMP) does incorporate viscous effects into an overall strip theory solution. Later on in this dissertation the frequency domain results of SMP will be used to generate a time history of

ship motions. The post processor for SAMP is then used to calculate the two components of pressure -- the cyclic hydrostatic pressure and the wave pressure (Froude-Krylov) -- that are based simply on the relative position of the ship and wave. These two components are a good estimate, especially at high wave frequencies, of total pressure on a panel.

In the use of SMP, the analysis must consider the non-linearity of roll motions in terms of wave height. In linear theory it is often considered that the frequency response of roll motions can be considered linear with wave height for a specific short term sea spectrum (one sea state, one wave heading one ship speed). For this sea spectrum an equivalent linear damping is computed and linear analysis proceeds. A comprehensive analysis thus requires a different load FTF for each sea state; this is the quasi-linear analysis discussed briefly in Chapter 1. However, the vast majority of fatigue occurs in the less severe sea states and roll response may be very nearly linear in this domain. For the Atigun Pass tanker studied in the example section, there was less than 5% difference in the response amplitude operators predicted by SMP for significant wave heights ranging between 1 and 7 meters. Full linear analysis was therefore performed.

Structural Analysis

The frequency domain transfer function of load generated above is a measure of the load caused by a unit amplitude wave vs. either wave frequency or encounter frequency. From the general field of spectral analysis, such transfer functions are often designated as $H_l^2(f)$, where

$$H_l^2(f) = \frac{S_l(f)}{S_w(f)} \qquad (4.2)$$

and

$S_l(f)$ is the load spectral density function

$S_w(f)$ is the wave spectral density function

As implied by the power of two, the frequency domain transfer function is actually the square of the load per unit wave height. In general a second transfer function must be determined, $H_\sigma^2(f)$, where

$$H_\sigma^2(f) = \frac{S_\sigma(f)}{S_l(f)} \tag{4.3}$$

$S_\sigma(f)$ is the stress spectral density function, or the response spectrum of stress.

By combining Equations 4.2 and 4.3, we get an expression for the frequency response spectrum of stress in terms of the load spectrum.

$$S_\sigma(f) = H_\sigma^2(f) H_l^2(f) S_w(f) \tag{4.4}$$

When the frequency of loading is very low relative to the natural frequency of the structural system, H_σ^2 is independent of frequency and can be considered a scalar.

$$S_\sigma(f) = H_\sigma^2 H_l^2(f) S_w(f) \tag{4.5}$$

All of the structural calculations performed in analyzing fatigue of a tanker fall within Equation 4.5. The structural analysis thus only requires the stress resulting from a unit static load. This is true for both hull girder bending and panel pressures. For simple geometries, such calculations require only basic structural analysis. If necessary due to structural geometry, such calculations can be performed using finite element analysis.

The fatigue assessment introduced in the next section does not explicitly use the response spectrum of stress, but rather the first four spectral moments, m_i.

$$m_i = \int_0^\infty f^i S(f) df$$

Fatigue Assessment

A design level method of fatigue damage assessment is most readily implemented using a full spectral analysis which incorporates: Miner's rule, S-N curves, a Rayleigh distribution of peak stress and a bandwidth adjustment factor. These concepts and their origins have been outlined in the previous chapter. Within this section, the explicit formula for fatigue damage in terms of the stress spectra will be derived.

In design oriented fatigue analysis, both the material properties of the structural member and the local stress concentration due to the joint type are incorporated into a series of S-N curves. The most comprehensive and widely available set of curves is that of the British Welding Institute [19]. Table 4.1 gives the parameters , defined in Equation 4.6, for this family of curves.

$$N(S_N)^m = C \qquad (4.6)$$

where: N is the number of cycles to failure

S_N is the failure stress level for N cycles

log(C) is the intercept of the cycles axis of the S-N curve

m is the negative slope of the S-N curve

Miner's rule of linear damage accumulation is

$$\eta_j = \sum_{i=1}^{B} \frac{n_{i,j}}{N_i} \tag{4.7}$$

where: η_j is the incremental damage ratio

i is for each incremental stress range

j is for each short term spectrum of load

The number of cycles in any stress range, n, can be associated with the probability of that stress range, p(s).

$$n_{i,j} = N_j p_j(s_i) ds \tag{4.8}$$

Thus Equation (4.7) is expressed as

$$\eta_j = \frac{N_j}{C}\left(\int S^m p_s(s) ds\right)_j = \frac{N_j}{C}\left[E\left(S^m\right)\right]_j \tag{4.8}$$

where: $E(S^m)$ is the expected value of S^m.

For the Rayleigh distribution, the probability density has the general form,

$$p_x(x) = \frac{x}{m_0} e^{\frac{-x^2}{m_0}} \tag{4.9}$$

where: m_i is the ith spectral moment of x

Performing the integration implied in Equation 4.8 and substituting for stress range yields

$$E\left(S^m\right) = \left(8m_0\right)^{m/2} \Gamma\left(1 + \frac{m}{2}\right) \tag{4.10}$$

where: $\Gamma()$ is the gamma function

Substituting back into Equation 4.8 results in fatigue damage as a function of spectral moments and number of cycles.

$$\eta_j = \frac{N_j}{C}(8m_0)^{m/2}\Gamma\left(1+\frac{m}{2}\right) \qquad (4.11)$$

For a narrow banded process the number of cycles in any short term spectrum j is

$$N_j = p(j)T_{life}f_{avg} \qquad (4.12)$$

where: p(j) is the total probability of occurrence of the short term spectrum

T_{life} is the design life for fatigue in seconds

$$f_{avg} = \sqrt{\frac{m_2}{m_0}}$$

Therefore the explicit fatigue damage ratio strictly in terms of S-N parameters and spectral moments for a narrow banded process is:

$$\eta_j = \frac{p(j)T_{life}}{C}\left(\frac{m_0}{m_2}\right)^{1/2}(8m_0)^{m/2}\Gamma\left(1+\frac{m}{2}\right) \qquad (4.13)$$

Equation 4.12 is strictly valid only for processes which are narrow banded. Alternative methods for counting the number of cycles of stress in non-narrow banded systems exist. One such method, the rainflow method by Masuishi and Endo [29], is highly recommended for wide band processes. The true rainflow method requires the full time history of stress and is therefore impractical for the current analysis method. Wirsching has instead developed an empirical rainflow correction factor λ, that is used to modify the results normally computed by the narrow band method. He has shown this adjustment factor to be particularly useful in the relatively narrow banded marine wave environment [22].

$$\lambda(m,\varepsilon) = a(m) + [1 - a(m)](1 - \varepsilon)^{b(m)} \tag{4.14}$$

where:

$$a(m) = 0.926 - 0.333m$$

$$b(m) = 1.587m - 2.323$$

$$\varepsilon = \sqrt{1 - \frac{m_2^2}{m_0 m_4}}$$

Thus the equation of incremental damage ratio used throughout this study is

$$\eta_j = \lambda \frac{p(j)T_{life}}{C} \left(\frac{m_0}{m_2} \right)^{1/2} (8m_0)^{m/2} \Gamma\left(1 + \frac{m}{2}\right) \tag{4.15}$$

Table 4.1: The Welding Research Institute S-N Parameters

Joint	log C (for N/mm^2)			log C (for psi)			m
Class	Mean	-1 SD	-2 SD	Mean	-1 SD	-2 SD	
B	15.37	15.19	15.01	24.02	23.84	23.65	4.0
C	14.03	13.83	13.63	21.60	21.40	21.19	3.5
D	12.60	12.39	12.18	19.09	18.88	18.67	3.0
E	12.52	12.27	12.02	19.00	18.75	18.50	3.0
F	12.24	12.02	11.80	18.72	18.50	18.29	3.0
F2	12.09	11.86	11.63	18.58	18.35	18.12	3.0
G	11.75	11.57	11.39	18.24	18.06	17.88	3.0
W	11.57	11.38	11.20	18.05	17.87	17.68	3.0
X			14.57			23.43	4.1

Note: Often only the column of -2 standard deviations is reported (-2 SD). These are the values appropriate for design. The mean values were used throughout this project so that the computed fatigue life would be comparable with that actually observed in service.

Chapter 5: Examples from Atigun Pass

Introduction

In the following chapter, three sample members from the Exxon Benicia will be analyzed. This analysis will demonstrate the level of effort that is reasonable for the vast number of structural members which must be sized during preliminary design. Although it is important that the results accurately demonstrate the fatigue life of a typical member with typical connection details, the intent is not to predict the precise fatigue life of a specific design detail or modification to such detail. For a precise evaluation of in-service details the reader is directed to the work of either the University of California at Berkeley Ship Maintenance Project [26] or Sucharski and Cheung [9].

The selection of members analyzed in this chapter includes a waterline longitudinal (L42), a lower side longitudinal (L30) and a typical bottom longitudinal (L10). All three are pictured in the cross section of Figure 5.1. Cracking for both side shell longitudinals is assumed to originate in the web at the toe of the transverse frame bracket. For the bottom longitudinal, cracking in the web to shell plating weld in the way of a limber hole is considered.

The first set of analyses will consider the case of head seas. Head seas are often used in the structural analysis of ships because of the extreme hull girder bending loads that result. Head seas also have the advantage that the predominant ship motions, heave, surge and pitch, are linear with wave height and can be accurately predicted using the potential flow

program SAMP. For the head seas case the analysis will be performed considering both the global hull girder bending loads and local panel pressures.

In order to better demonstrate the lifetime fatigue damage contribution due to panel pressures, a second analysis will be performed for three relative wave headings: head, bow quarter and beam. These analyses will substitute the US Navy's Ship Motions Program (SMP) for SAMP and calculate an estimate of panel pressures.

The following data, describing a February 1992 voyage from Valdez to San Francisco, will be used for all example calculations.

V_{ship} = 15 knots
Draft = 50 ft
Light Ship = 24707 LT
Displacement = 168956 LT
L_{cg} (from A.P.) = 456.16 ft
V_{cg} (above keel) = 40.73 ft

The following mass moments were estimated based on the known cargo load and an assumed distribution of the light ship mass:

$$I_{xx} = 3.65 \times 10^{11} \ \frac{\text{lb-sec}^2}{\text{in}}\text{-in}^2$$

$$I_{yy} = 5.65 \times 10^{12} \ \frac{\text{lb-sec}^2}{\text{in}}\text{-in}^2$$

$$I_{zz} = 5.71 \times 10^{12} \ \frac{\text{lb-sec}^2}{\text{in}}\text{-in}^2$$

5.1 Example 1: Panel Pressure, Lower Side Longitudinal (L30)

Longitudinal 30 is in the lower side shell approximately 97" above the baseline. Because longitudinal 30 is in the side shell and at a significant distance from the hull's neutral axis, it is reasonable to expect fatigue damage due to both panel pressure fluctuations and hull

girder bending. The example considers the welded joint between the outer edge of the web of the side longitudinal and the flat bar bracket at a typical web frame (see Figure 2.4). The first example calculation computes the contribution of local pressure fluctuations to fatigue damage. Example 2 will examine fatigue damage due to hull girder bending at this same location. Since the purpose is simply to illustrate the method, both calculations are done for only one heading.

Pressure Transfer Function

A single transfer function, $H^2(f_e)$, is required for this calculation. Due to the energy content of the wave environment, a transfer function throughout the range $f_w = 0.04$ to 0.20 Hz is sufficient. The panel geometry used for the hydrodynamic analysis uses 207 panels to describe the submerged portion of the hull. Time histories of panel pressures, see for example Figure 5.2, are calculated for a series of regular waves using the linear hydrodynamics program SAMP and a post processor supplied with SAMP which interpolates pressures for any desired point on the hull surface. The SAMP runs use the following parameters:

15 values of f_w from 0.04 to 0.20 Hz

Wave Amplitude = 72 in

For each time history a Fast Fourier Transform (FFT) was performed to determine the pressure response amplitude at wave encounter frequency. The quantity

$$\left(\frac{P_{amp}}{Wave_{amp}}\right)^2$$

is plotted against wave frequency. The result is Figure 5.3, a transfer function for panel pressure.

Stress Transfer Function

For the relatively low frequency pressure fluctuations normally considered, a static stress analysis is sufficient. The overall fatigue analysis method proposed herein normally uses MAESTRO on a PC or workstation to rapidly generate a whole ship structural model, and to obtain representative or "field" stresses in all principal structural members (but not hotspot stresses). This enables the analyst to accurately assess member field stresses for a given load with the assurance that the local boundary conditions are complete and correct. However, even this simple PC-based analysis was not required for the side longitudinals considered herein, because each segment between transverse frames is nothing more than a clamped beam subjected to a uniform distributed load. Therefore stress levels in the outer edge of the web were calculated using beam theory, allowing for the asymmetry of the flange (Appendix B provides the details of the stress analysis for all members). The resulting transfer function

$$\left(\frac{\sigma_{amp}}{Wave_{amp}}\right)^2$$

is given by Figure 5.4.

Wave Spectrum

The TAPS Tanker route and the location of the four buoys which have been chosen to describe the wave environment are shown in Figure A-1 of Appendix A. The length of the route defined by each buoy was scaled from the map and divided by total route length to compute the location probabilities in Table 5.1.

The wave spectra for the buoys are calculated based on the Ochi parameters given in Appendix A. Shown in Figure 5.5 is the wave frequency spectrum for Buoy 46002 at H_{m_o} = 4.0 m and Figure 5.6 is the encounter frequency spectrum. The comparison of the two figures demonstrates the importance of the encounter frequency modification.

Response Spectrum

For each sea state of concern, H_{m_o}= 1.0 to 13.0 m, the transfer function H_σ^2 is multiplied by the respective wave spectrum $S_W(f_e)$. The spectral moments, m_0 and m_2, of the resulting response spectrum $S_\sigma(f_e)$ are then calculated. As an illustration of the intermediate results, a single response spectrum is given in Figure 5.7.

Damage Ratio

The damage ratio, η, is calculated by combining the response spectral moment, m_0 with the parameters C and m (which describe an S-N curve) in Equation 16. The values of C and m are based on the joint classification system of the Welding Institute [19]. For the bracketed end connection of the side shell longitudinals to the transverse web frame, the joint type is 4.2 and the classification is G. The S-N curve parameters are thus, C = 1.738×10^{18} and m = 3.0. The operating lifetime used in the example is T_{life} = 20 years and the probability associated with each response spectrum is calculated in Table 5.2.

The response spectrum probabilities of Table 5.2, the spectral moments and the fatigue strength parameters are all combined to compute the fatigue damage ratio of a single spectrum. Table 5.3 shows the contribution to η for 11 different sea states. Each contribution represents only the damage accumulated during a single sea state, location, draft, heading and speed combination.

5.2 Example 2: Hull Girder Bending, Lower Side Longitudinal (L30)

This example demonstrates the technique used to calculate fatigue damage due to hull girder bending at the same location as in Example 1. The resulting damage can thus be algebraically added to the results from the panel pressure analysis. The operating condition for this example is again: loaded, forward speed of 15 knots and head seas. The wave spectra are also identical. The transfer function for this particular operating condition is given in Figure 5.8.

To demonstrate the difference between hull girder and panel pressure response, we examine Figures 5.4 and 5.8 which give the frequency response transfer function of stress in a side shell longitudinal due to both. Each of the transfer functions has a distinct peak which essentially corresponds to a peak in the overall ship motion response. The transfer function for hull girder bending, however, has a much steeper decay. For example, at fe = 0.2 Hz the value of the response function for pressure is still at 25% of its peak value whereas the value for hull bending moment is at 1%. The discrepancy between the two types of transfer functions becomes even greater for members near the mean waterline. Because the basic nature of the two transfer functions is quite different, it is impossible to accurately derive the function for panel pressure by scaling the function for midship bending moment, which has been proposed (see for instance [30]).

As in Example 1, the joint type is 4.2, the class is G and the S-N curve parameters are $C = 1.738 \times 10^{18}$ and m = 3.0. The fatigue damage ratio for each sea state is summarized in Table 5.4. Again the total from Table 5.4 represents the contribution to the fatigue damage ratio due to hull girder bending for a single operating condition and a single buoy location. A complete analysis would proceed to evaluate all other operating headings as

well as each buoy location, but as explained earlier, it is not yet possible to obtain results for all headings.

5.3 Example 3: Panel Pressure, Midheight Side Longitudinal (L42)

Longitudinal 42 is located approximately at the ship's design water line and thus panel pressures do not decay as quickly, in comparison to longitudinal 30, with wave frequency. It should also be noted that longitudinal 42 is designed for a smaller hydrostatic head than longitudinal 30 and accordingly a smaller cross sectional area is used. The result is higher stresses in longitudinal 42 for equivalent panel pressures. Figure 5.9 shows the encounter frequency transfer function of outer web stress for L42.

The stress value for longitudinal 30 starts at a relatively low value and decays to an insignificant quantity within the frequency range of significant wave energy. However, the transfer function for longitudinal 42 starts at a large value and remains significant throughout the frequency range. The fatigue analysis for longitudinal 42 is performed in an identical manner to that shown for longitudinal 30. The joint type and class are again 4.2 and G, respectively. The pertinent data for the calculation are given in Table 5.5.

The final result of Table 5.5 is a damage ratio of 0.068, or 25 times the damage due to pressure in longitudinal 30 for the same operating condition. This value is for 1 out of 64 lifetime operating conditions and therefore represents a significant contribution towards a possible fatigue failure. For both longitudinals 30 and 42, other headings involve much more rolling, and rolling can typically increase the time-varying dynamic component of pressure on a ship's side by a factor of two or more, depending on the degree of rolling.

It is also important to note that longitudinal 42 is near the ship's neutral axis. Any analysis procedure which relies exclusively on hull girder bending would predict little or no fatigue

damage to such a member. This example shows that fatigue damage due to panel pressures can be quite significant. Therefore it is clear that any rationally-based analysis or design procedure must consider not just hull girder bending, but also the dynamic panel pressures due to waves and ship motions, including roll.

5.4 Example 4: Bottom Longitudinal; Web to Plating Weld

The US Coast Guard follow-up report [8] stated that the Atigun Pass class was subject to various fractures of the bottom longitudinals in way of limber holes/erection butt welds. The shell bottom panels are not subject to significant wave frequency local panel pressures, so it is likely that the dominant cause of these fractures is hull girder bending. The following example will examine a typical shell bottom longitudinal in terms of hull girder bending.

Joint type 6.5, a class F joint, is specified for the end region of a web to flange weld. Included in the classification is the SCF for a small cope hole in the web. Table 5.6 details the results of the fatigue damage calculation. Again this calculation is computed for a single wave buoy location and ship heading.

Summary of SAMP Based Fatigue Calculations

The author has written several computer programs which automate the fatigue calculation. Through the use of this software, the calculations for examples 1 to 4 were repeated for the remaining 3 buoy locations. Table 5.7 summarizes the fatigue calculations for all of the buoy locations.

All of the examples have accumulated significant fatigue damage during just under 6% of their 20 year operating life. It appears that damage in L42 due to panel pressures and damage in L30 and a typical bottom longitudinal due to hull girder bending are of the same magnitude. It is tempting at this point to extrapolate beyond the 6% of operating life considered; for example 2, 0.015/0.06 = 2.5 or a fatigue life of 20/2.5 = 8 years. However, the fatigue lives calculated in this manner in Table 5.8 are simply bounds (either upper or lower as described below) on the fatigue life calculation.

The fatigue life given in the final column of Table 5.8 is labeled as a bound because of the ship heading considered. In the case of hull girder bending, the 6% of vessel life considered (head seas) leads to the maximum structural loads. Thus the extrapolated fatigue life is based on a worst case scenario and can be considered an upper bound. For panel pressures the magnitude of alternating pressures is minimum in head seas (in the absence of roll). In this case the extrapolated life is based on the best (least severe) 6% of ship life and is thus a lower bound. From such comparisons it is reasonable to expect that in a full analysis, panel pressures will be a significant concern. In the following section examples will be presented to clarify the importance of panel pressures.

Three-Heading Analysis

In the prior section fatigue analyses were performed for the 6% of ship life that involves head seas during a cargo voyage. To extend the analysis to a more representative cross section of the ship's life requires consideration of roll motions in response to wave loads. Although the current version of SAMP, the general 3-D hydrodynamics package used for the head seas analysis, is not capable of generating realistic roll damping forces, it is

possible to estimate panel pressures based on ship motions from the US Navy's Ship Motions Program (SMP).

The technique behind this estimation is covered in more depth in Chapter 4. In brief, SMP is used to determine the Response Amplitude Operator (RAO) for 6 degrees of freedom of ship movement. The RAO's are used to position and orient the ship within a regular wave. Two components of panel pressure are then easily computed. The first is the hydrostatic component, or the pressure due to the instantaneous depth of a panel center beneath the mean waterline. The second component of pressure, termed the Froude-Krylov, is the internal wave pressure due to the orbital motion of water particles. The third component of pressure, the perturbation effect of the ship on the wave, is omitted in this procedure. Figure 5.10 compares the panel pressures computed by SAMP and by using the 2-component estimate. Agreement between the two methods is good, especially at relatively high frequencies where the SAMP computation becomes quite expensive.

Examples 1 and 3 are reconsidered, but now for three wave directions: head, starboard-bow quarter and starboard beam. Again only the loaded condition is analyzed, but now the segment of ship's life considered is up to 24%. The results of both calculations are given in Table 5.9.

Extending the analysis beyond head seas further demonstrates the importance of panel pressures. Now the predicted fatigue life for longitudinal 42 is substantially shorter than even the worst of the hull girder dominated fatigue lives. For L30 the 20 year damage ratio for panel pressures is approaching 1, which means that there is little fatigue life available for the locally more severe case of hull girder bending.

Summary of Results

Three specific structural members have been analyzed for fatigue. In all cases the members were found to have fatigue lives substantially shorter than projected ship life. Since in all three cases substantial numbers of fatigue cracks have appeared in under 10 years, the analysis performed would have been of great benefit if performed during preliminary design. Most significantly, the analysis of the waterline longitudinals, for which hull girder fatigue analysis predicts almost no damage, predicts a fatigue life of just over 3 operating years.

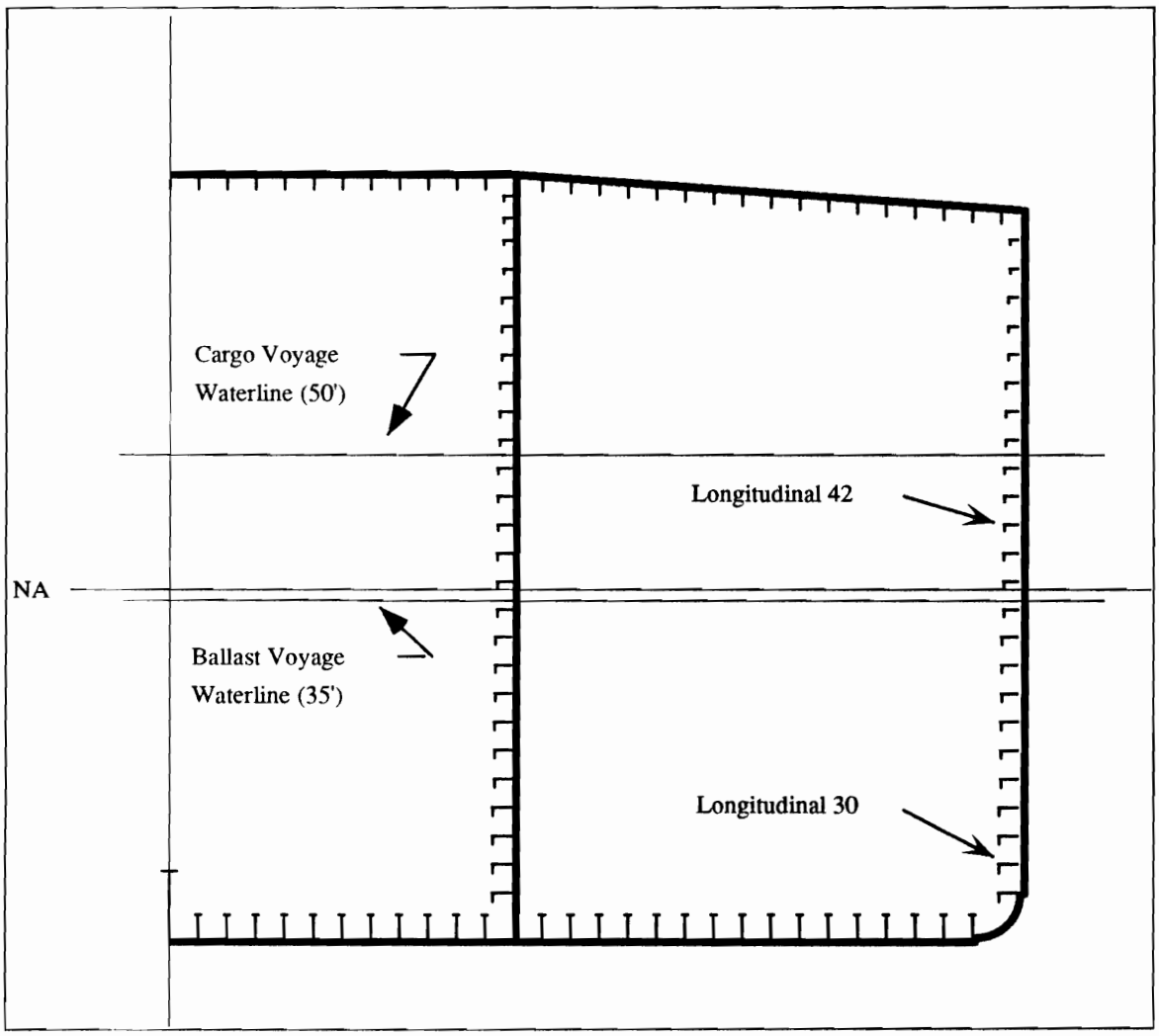

Figure 5.1: Cross Section of Atigun Pass Parallel Midbody

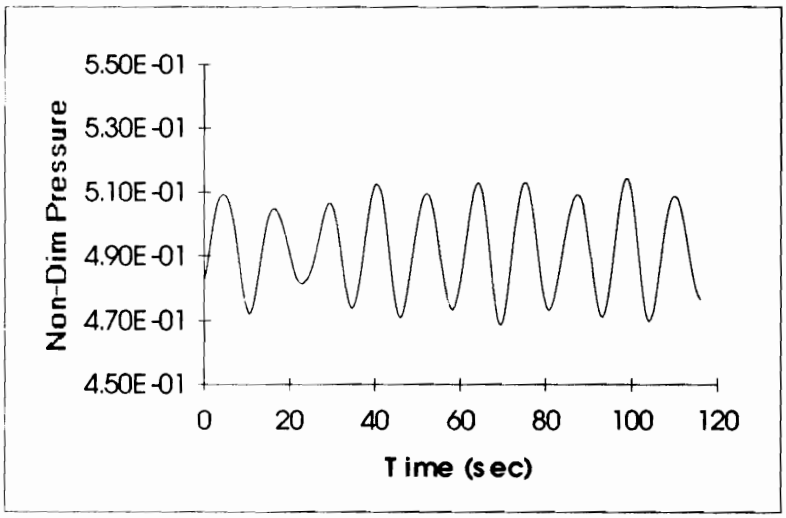

Figure 5.2: Pressure time history for Longitudinal 30 at midships due to head seas.

Note: Pressure is presented in non-dimensional form, $p/(\rho g l)$. Relevant parameters are: V_{ship} = 15 knots, f_{ω} = 0.06 Hz and time step = 0.50 seconds.

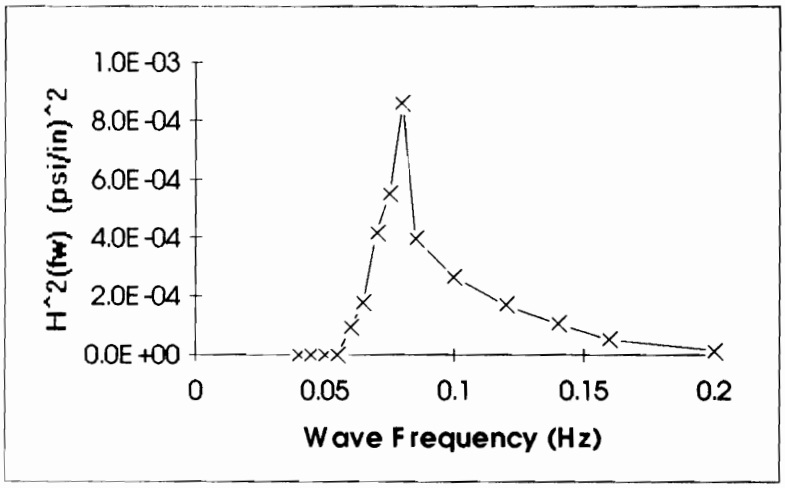

Figure 5.3: Panel pressure transfer function for Longitudinal 30

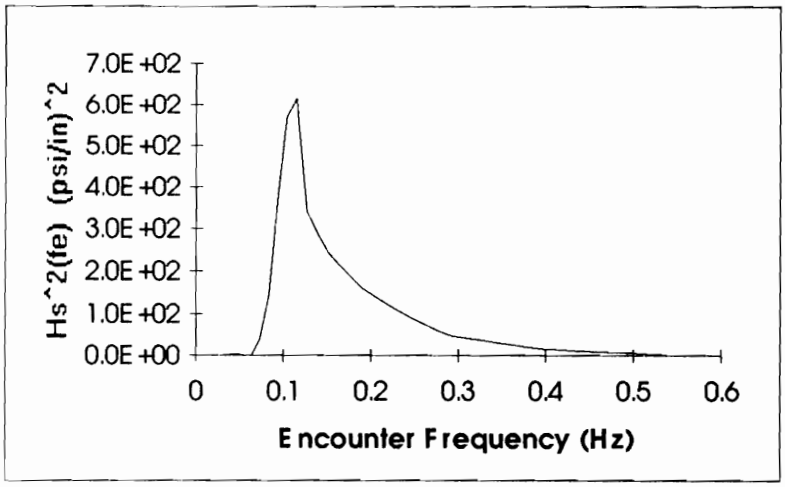

Figure 5.4: Stress transfer function for Longitudinal 30

Note: Both transfer functions are for a forward speed of 15 knots and head seas.

Table 5.1: Location Probabilities for 4 buoys along the TAPS route

Buoy	P(loc)
46001	0.32
46004	0.26
46005	0.14
46002	0.28

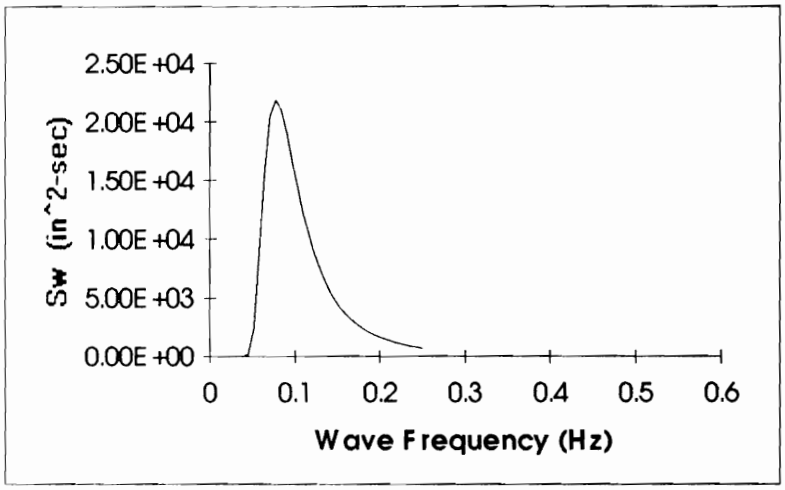

Figure 5.5: Wave frequency spectra for West Coast Long Period Seas.

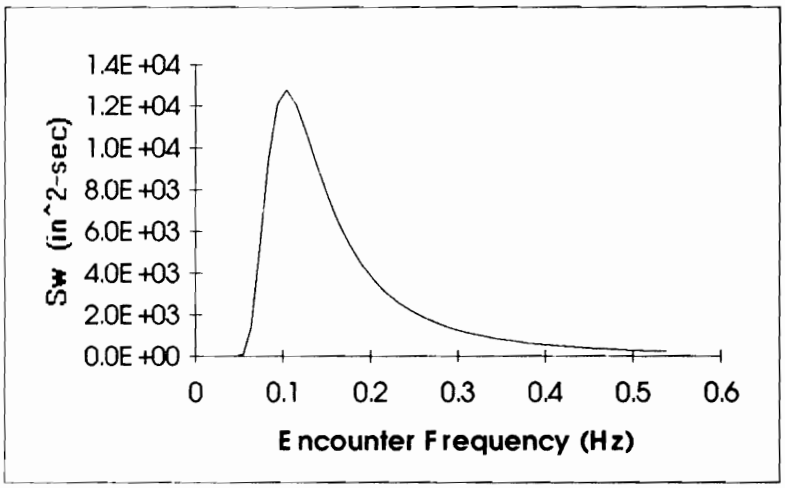

Figure 5.6: Encounter frequency spectra for West Coast Long Period seas.

Note: For both Figures 5.5 and 5.6 the location is NOAA buoy 46002 and Significant wave height is 4 meters.

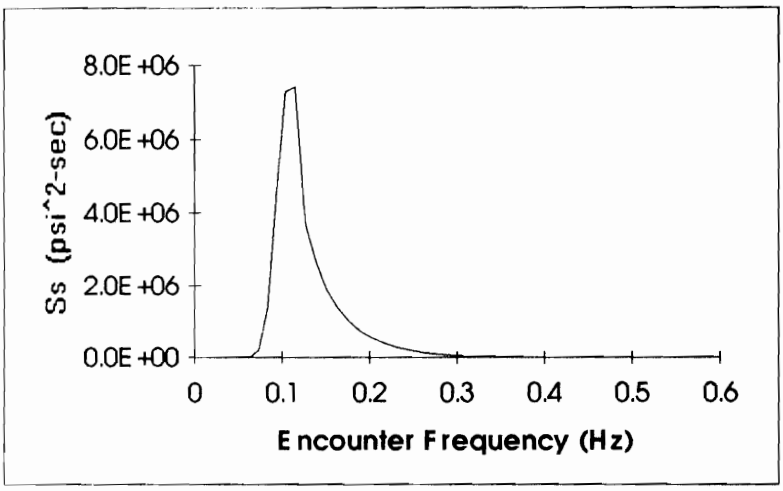

Figure 5.7: The stress response spectrum, $S_{\sigma}(f_e)$, for L30

Note: Again the parameters for Figure 5.7 are: head seas, buoy 46002, 15 knots, Hmo = 4.0 meters and cargo voyage.

Table 5.2: Response Spectra Probabilities for Buoy 46002

Hm_0	$P(V_{ship})$	$P(\theta)$	P(Draft)	$P(Hm_0)$	P(loc)	P(RSP)
1	1	0.055	0.5	0.1905	0.28	1.47E-03
2	1	0.0615	0.5	0.3171	0.28	2.73E-03
3	1	0.1055	0.5	0.2323	0.28	3.43E-03
4	1	0.123	0.5	0.1455	0.28	2.51E-03
5	1	0.1005	0.5	0.0667	0.28	9.38E-04
6	1	0.0925	0.5	0.0278	0.28	3.60E-04
7	1	0.099	0.5	0.0113	0.28	1.57E-04
8	1	0.077	0.5	0.0042	0.28	4.53E-05
9	1	0.056	0.5	0.0028	0.28	2.20E-05
10	1	0	0.5	0.0007	0.28	0.00E+00
>10.0	1	0	0.5	0.0007	0.28	0.00E+00

Note: head seas and cargo voyage draft.

Table 5.3: Fatigue damage ratios for L30 due to panel pressures.

Hm_o	m_0	m_2	m_4	P(RSP)	ε	η
1	3.55E+04	1.16E+03	6.74E+01	1.47x10-3	0.661898	1.63E-05
2	1.81E+05	5.13E+03	2.62E+02	2.73x10-3	0.667673	3.24E-04
3	2.05E+05	4.22E+03	1.50E+02	3.43x10-3	0.646851	4.19E-04
4	3.92E+05	7.30E+03	2.32E+02	2.51x10-3	0.643437	7.70E-04
5	6.20E+05	1.08E+04	3.19E+02	9.39x10-4	0.639653	5.56E-04
6	8.78E+05	1.47E+04	4.11E+02	3.60x10-4	0.63598	3.51E-04
7	1.16E+06	1.87E+04	5.03E+02	1.57x10-4	0.632916	2.27E-04
8	1.45E+06	2.28E+04	5.97E+02	4.53x10-5	0.630053	9.13E-05
9	1.75E+06	2.71E+04	6.92E+02	2.20x10-5	0.627733	5.83E-05
10				0.00E+00		0
>10.0				0.00E+00		0
					Total	2.81E-03

Note: Parameters are: Buoy 46002, $\theta = 180$ and Draft = 600 in.

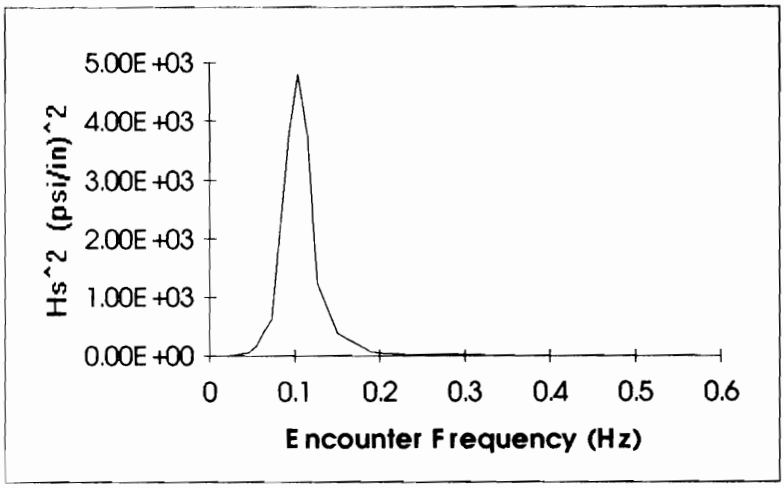

Figure 5.8: Hull girder bending moment stress transfer function for L30 at midships.

Table 5.4: Fatigue damage ratios for L30 due to hull girder bending.

Hm_0	m_0	m_2	m_4	P(RSP)	ε	η
1	1.13E+05	1.72E+03	4.08E+01	1.47x10-3	0.598414	6.39E-05
2	6.98E+05	9.83E+03	2.00E+02	2.73x10-3	0.55406	1.76E-03
3	1.02E+06	1.31E+04	2.07E+02	3.43x10-3	0.436334	3.82E-03
4	2.23E+06	2.68E+04	3.91E+02	2.51x10-3	0.417658	8.74E-03
5	3.83E+06	4.42E+04	6.11E+02	9.39x10-4	0.408281	7.22E-03
6	5.73E+06	6.42E+04	8.58E+02	3.60x10-4	0.403385	5.00E-03
7	7.89E+06	8.62E+04	1.12E+03	1.57x10-4	0.401232	3.47E-03
8	1.02E+07	1.10E+05	1.40E+03	4.53x10-5	0.400296	1.47E-03
9	1.27E+07	1.34E+05	1.69E+03	2.20x10-5	0.400473	9.80E-04
10				0.00E+00		0
>10.0				0.00E+00		0
					Total	3.25E-02

Note: Parameters are: Buoy 46002, θ = 180 and Draft = 600 in.

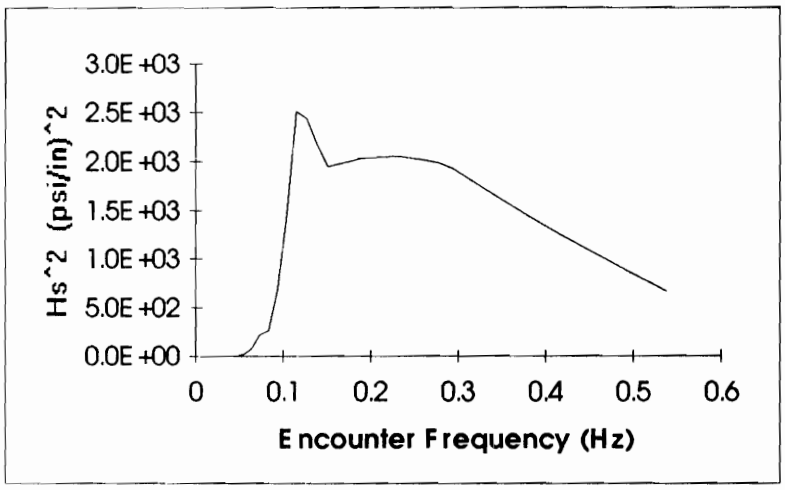

Figure 5.9: Stress transfer function due to pressure for Longitudinal 42

Note: Forward speed of 15 knots and head seas.

Table 5.5: Fatigue damage ratios for L42 due to panel pressures.

Hmo	m0	m2	m4	P(RSP)	e	h
1	4.41E+05	2.88E+04	3.10E+03	1.47E-03	0.628125	1.01E-03
2	1.90E+06	1.09E+05	1.06E+04	2.73E-03	0.643044	1.57E-02
3	1.48E+06	5.89E+04	4.73E+03	3.43E-03	0.70912	1.12E-02
4	2.49E+06	8.95E+04	6.73E+03	2.51E-03	0.722133	1.70E-02
5	3.64E+06	1.22E+05	8.73E+03	9.39E-04	0.730197	1.08E-02
6	4.88E+06	1.55E+05	1.07E+04	3.60E-04	0.735664	6.30E-03
7	6.18E+06	1.88E+05	1.27E+04	1.57E-04	0.739675	3.82E-03
8	7.54E+06	2.22E+05	1.46E+04	4.53E-05	0.742626	1.46E-03
9	8.93E+06	2.57E+05	1.66E+04	2.20E-05	0.744811	9.03E-04
10				0.00E+00		0
>10.0				0.00E+00		0
					Total	6.83E-02

Note: Buoy 46002, $\theta = 180$ and Draft = 600 in.

Table 5.6: Fatigue damage ratios for typical bottom longitudinal due to hull girder bending moment.

Hmo	m0	m2	m4	P(RSP)	e	h
1	1.81E+05	2.78E+03	6.91E+01	1.47E-03	0.619585	4.29E-05
2	1.12E+06	1.58E+04	3.32E+02	2.73E-03	0.570982	1.18E-03
3	1.64E+06	2.10E+04	3.36E+02	3.43E-03	0.447151	2.55E-03
4	3.57E+06	4.30E+04	6.32E+02	2.51E-03	0.426211	5.85E-03
5	6.13E+06	7.07E+04	9.86E+02	9.39E-04	0.415419	4.83E-03
6	9.17E+06	1.03E+05	1.38E+03	3.60E-04	0.410616	3.35E-03
7	1.26E+07	1.38E+05	1.81E+03	1.57E-04	0.406642	2.32E-03
8	1.64E+07	1.76E+05	2.26E+03	4.53E-05	0.405002	9.84E-04
9	2.04E+07	2.15E+05	2.72E+03	2.20E-05	0.405236	6.56E-04
10				0.00E+00		0
>10.0				0.00E+00		0
					Total	2.18E-02

Note: Buoy 46002, $\theta = 180$ and Draft = 600 in.

Table 5.7: Summary of fatigue damage calculation for all four wave buoys.

Ex	Description	η at Buoy Number				Total	
		46001	46002	46004	46005	p(occ)	η
1	L30 Panel Pressure	5.0E-03	2.8E-03	5.0E-03	1.5E-03	5.8E-02	1.4E-02
2	L30 Hull Girder	5.0E-02	3.3E-02	5.1E-02	1.8E-02	5.8E-02	1.5E-01
3	L42 Panel Pressure	1.2E-01	6.8E-02	1.2E-01	3.6E-02	5.8E-02	3.5E-01
4	BL Hull Girder	3.4E-02	2.2E-02	3.4E-02	1.2E-02	5.8E-02	1.0E-01

Note: Other parameters restricted to head seas and cargo voyage. The column p(occ) is the fraction of the 20 year life being considered for η total.

Table 5.8: Estimates of fatigue life based on calculations covering 6% of 20 year life

Ex.	Description	Total		Extrap.	Life	Adj	Bounds
		p(occ)	η	η	(year)		(year)
1	L30 Panel Pressure	5.8E-02	1.4E-02	0.2471			
2	L30 Hull Girder	5.8E-02	1.5E-01	2.628	7.0	1	7.0
3	L42 Panel Pressure	5.8E-02	3.5E-01	6.0147	3.3	2	6.7
4	BL Hull Girder	5.8E-02	1.0E-01	1.7587	11.4	1	11.4

Note: Extrapolated η is computed by dividing the total η calculated by the percentage of 20 year life considered. Fatigue life in years is found by dividing the extrapolated η into a 20 year life. Example 3 contains an adjustment factor because L42 is actually above the waterline during ballast voyages and accumulates no damage during this time period.

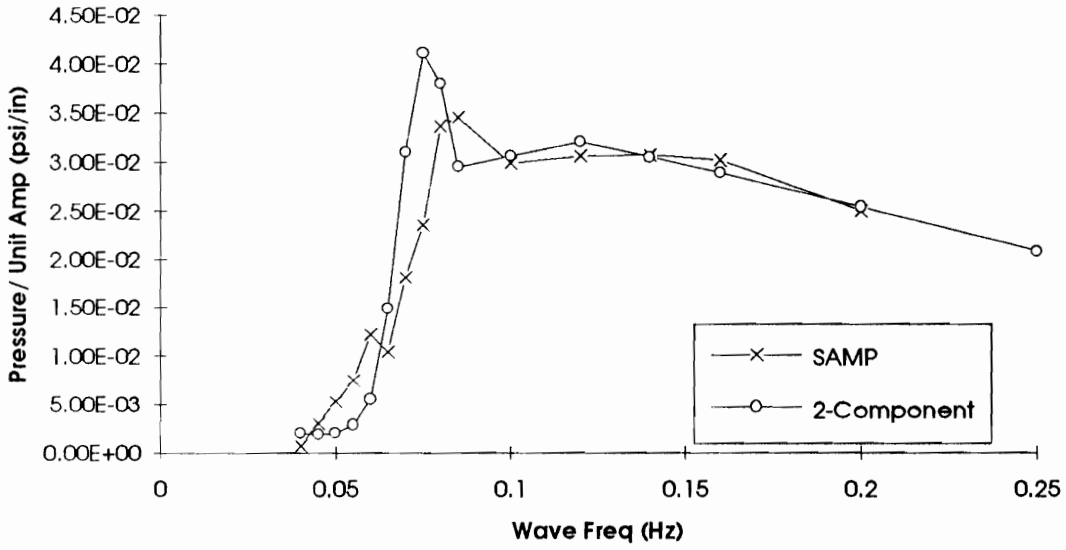

Figure 5.10: Comparison of SAMP panel pressure and a 2-component estimate.

Table 5.9: Results of 2-component analysis.

Ex.	Member	Head Sea η	Quarter Sea η	Beam Sea η	Total η	P(occ)
1	L30	.026	.067	.089	0.182	0.24
3	L42	.409	.651	1.782	2.84	0.24

Table 5.10: Extrapolated results of 2-component analysis.

Ex.	Member	Extrap. η	Extrap Life (year)	Adj.	Expected Life (year)
1	L30	0.77	26	1	26
3	L42	12.0	1.7	2	3.3

Note: Estimates of fatigue life based on covering 24% of 20 year ship life. Extrapolated η is computed by dividing the total η calculated by the percentage of 20 year life considered. Fatigue life in years is found by dividing the extrapolated η into a 20 year life. Example 3 contains an adjustment factor because L42 is actually above the waterline during ballast voyages and accumulates no damage during this time period.

Chapter 6: Conclusions

The costly and well publicized fatigue fractures which have occurred in the TAPS tankers have concentrated considerable attention on the topic of ship structural fatigue. Several research efforts have been initiated to evaluate the in-service life of various structural details and generate retro-fit solutions. Other costly repercussions of the TAPS fatigue problem include the extra regulatory effort required by the US Coast Guard and additional operating costs incurred by owners and operators.

In response to these costs, it seems assured that some level of fatigue design will be required for the generation of tankers yet to be built. In order to avoid a lengthy trial and error process, it is critical for the ship structures community to develop an informed consensus about the makeup of any such new design technique.

The greatest amount of effort that is currently being expended on fatigue analysis is for the in-service fatigue life of specific design details. Such calculations are expensive and incorporate elegant FE models. These studies also tend to be well funded; for many tanker operators the performance of the existing fleet is paramount. The economics of spending a few engineering dollars to save many in operations (in a relatively short time) has been relatively easy to sell.

This project has, however, dealt with a slightly different issue. Can preliminary design, and thus the subsequent stages of detail design and operations/maintenance, benefit from

inexpensive fatigue life calculations? If the answer is yes, what level of effort is required? Are there factors in such an analysis which may be overlooked?

It is evident from the results presented in Chapter 5, that some of the current TAPS tankers would have benefited substantially from a preliminary design analysis that included fatigue. Improving the connection details will give some increase in the fatigue life of various connections within these ships, but it will not cure the problem. The cyclic member stress levels which currently result in a fracture every 3 to 5 years will continue to lead to unacceptable levels of fatigue damage.

For new ships the balance between detail and preliminary design becomes even more evident. Just one aspect is the ability to compare the cost between increasing member scantlings and improving detail design and construction practices. An additional aspect is the design incorporation of robustness; a design that concentrates strictly on a minimum SCF for fatigue control will be very susceptible to fatigue failures caused by localized imperfections (either construction defects or post construction changes such as corrosion and modifications).

Also evident from Chapter 5 is that fatigue analysis as a simple extension of extreme load analysis is not sufficient. Many of the existing tanker fatigue studies have concentrated on global effects such as hull girder bending. This is a direct influence of traditional extreme load calculations, where simple hull girder calculations have been used to determine the mid-body cross section.

In contrast to the emphasis on hull girder bending, this study shows that there is significant fatigue damage in the side shell due to panel pressures. These panel pressures are not as commonly computed as hull girder bending moments, but there have been recent and

substantial improvements in the required computational methods. Continued improvements in such hydrodynamic load methods should be pursued with the aim of delivering a comprehensive and ready-to-use package to the ship structures community.

In summary, complete and effective fatigue design should be a two part process. During preliminary design effort should be expended to ensure cyclic member stresses are at levels for which unreasonable detail design will not be required. The detail design process must establish serviceable connection details with values of SCF that result in the desired fatigue resistance. In both levels of design, all significant sources of alternating structural loads must be considered. Preliminary fatigue design including relatively inexpensive consideration of local and global loads is both possible and necessary.

References

1. *Report on the Trans-Alaska Pipeline Service (TAPS) Tanker Structural Failure Study*, United States Coast Guard Report, June 25, 1900.

2. Radaj, Dieter, *Design and Analysis of Fatigue Resistant Welded Structures*, Halsted Press, New York, NY, 1990.

3. Chen, Y.N. and Mavrakis, S.A., "Closed-Form Spectral Analysis for Compliant Offshore Structures", *Journal of Ship Research*, **32** (4), Dec. 1988, pp. 297-304.

4. Rutherford, S.E. and Cladwell, J.B., "Ultimate Longitudinal Strength of Ships: A Case Study", *SNAME Annual Meeting 1990*, SNAME, Jersey City, NJ, 1990.

5. Lacey, P. and Edwards, R., "ARCO Tanker Slamming Study," *Marine Technology*, **30** (3), July 1993, pp. 135-147.

6. Hughes, O.F., *Ship Structural Design, A Rationally-Based, Computer-Aided, Optimization Approach*, SNAME, Jersey City, NJ, 1988.

7. Lin, W. and Yue, D., "Numerical Solutions for Large-Amplitude Ship Motions in the Time Domain", *The Eighteenth Symposium on Naval Hydrodynamics*, University of Michigan, Ann Arbor Michigan, August 19, 1990.

8. *Trans-Alaska Pipeline Service (TAPS) Tanker Structural Failure Study, Follow-Up Report*, United States Coast Guard Report, May 1991.

9. Sucharski, D. and Cheung, M.C., "Applications of Spectral Fatigue Analysis to the ARCO 190 Mdwt Tankers", *Proceedings, Ship Structure Symposium '93*, SNAME/SSC, Jersey City, NJ, Nov. 1993.

10. St. Denis, M. and W.J. Pierson, "On the Motions of Ships in Confused Seas," *Trans. SNAME*, **61**, 1953.

11. Buckley, W.H., "The Determination of Ship Loads and Motions: A Recommended Engineering Approach," *Naval Engineers Journal*, May 1990, pp. 209-227.

12. Hogben, N. and F.E. Lumb, *Ocean Wave Statistics*, National Physical Laboratory, H. M. Stationery Office, London, 1967.

13. Walden, H., "Die Eigenchaften der Meerswellen in Nordatlantischen Ozean," *Deutscher Wetterdienst, Einzelveroffentlichungen*, No. 14, 1964 (in German).

14. Cummins, W.E., S.L. Bales and D.M. Gentile, "Hindcasting Waves for Engineering Applications," *Proceedings of the Symposium on Hydrodynamics in Ocean Engineering*, Norwegian Hydrodynamic Laboratories, Trondheim, Norway, 1981.

15. Meyers, W.G., Applebee, T.R. and Baitis, A.E., "Users Manual for the Standard Ship Motion Program, SMP", DTNSRDC Report SPD-0936-01.

16. Lin, W. and Meinhold, M.J. "SAMP/LAMP Small Amplitude Motions Program and Large Amplitude Motions Program, Version 2.1", SAIC Marine Hydrodynamics Division, Annapolis, MD, Sept. 27, 1993.

17. Palmgren, A., "Die Lebenstauer von Kugellagern," ZVDI, **68**, 1924, p. 339.

18. Miner, M.A., "Cumulative Damage in Fatigue," *Journal of Applied Mechanics*, **12**, 1945, p. A-159.

19. *Welding Institute Research Bulletin*, 17 (5), May 1976.

20. Gurney, T.R., *Fatigue of Welded Structures*, Cambridge University Press, Cambridge, 1979.

21. Rice, O., "Mathematical Analysis of Random Noise," *Bell Systems Technology Journal*, **23**, 1944.

22. Wirsching, P.H., "Fatigue Reliability for Offshore Structures", *Journal of Structural Engineering*, **110** (10), Oct, 1984, pp. 2340-2356.

23. Wirsching, P.H. and Light, M.C., "Fatigue Under Wide Band Random Stresses", *Journal of Structural Engineering*, **106** (7), July, 1980, pp. 1593-1607

24. Sikora, J., Dinsenbacher, A. and Beach, J., "A Method for Estimating Lifetime Loads and Fatigue Lives for Swath and Conventional Ships", *Naval Engineers Journal*, May 1983.

25. *Recommended Practice for Planning, Designing and Constructing Fixed Offshore Platforms, 19th Edition, (API RP-2A)*, American Petroleum Institute, August 1, 1991.

26. *Structural Maintenance for New and Existing Ships*, Reports SMP-1-5 through 5-1, Department of Naval Architecture and Offshore Engineering, University of California at Berkeley, September, 1992.

27. *Guide for the Fatigue Strength Assessment of Tankers*, American Bureau of Shipping, New York, NY, 1992.

28. Capanoglu, C., *Fatigue Technology Assessment and Strategies for Fatigue Avoidance in Marine Structures*, SSC-367, Ship Structures Committee, Washington, DC, 1993.

29. Matsuishi, P.W., and Endo, T., "Fatigue of Metals Subjected to Varying Stress," presented at 1968, Japan Society of Mechanical Engineers, Fukuoka, Japan.

30. Liu, D., Itoh, T., Kawachi, S., Shigematsu, K., "Dynamic Load Approach in Tanker Design," *SNAME Annual Meeting 1992*, SNAME, Jersey City, NJ, 1992.

Appendix A: Wave Buoy Data

Figure A-1 identifies the four NOAA buoy stations at which percentage occurrence of H_{mo} and wind direction data have been obtained for the TAPS route. Also shown are the two generalized wave climates for which climatic wave spectra are discussed in Tables A-3 and A-4.

Tables A-1,-2 give the percentage occurrence of significant wave heights at each of the four buoy stations.

Table A-3 provides the Ochi (3P) spectrum approximations to the CWS of the Northern High Latitude wave climate area of Figure A-1.

Table A-4 provides the Ochi (3P) spectrum approximations to the CWS of the Long Period wave climate area of Figure A-1. In this case multiple Ochi (#3P) wave spectrum approximations are recommended for use for H_{mo} = 1 and 2 meters.

Tables A-5, -6,-7,-8 provide approximate seaway directionality information based upon percentage occurrence of wind direction *vs.* H_{mo} at each of the four buoy stations. The tanker route was estimated to be about 24 degrees off the latitude grid. It was convenient to use 22.5 degrees in defining the ship route and 45 degrees in defining class intervals of ship heading.

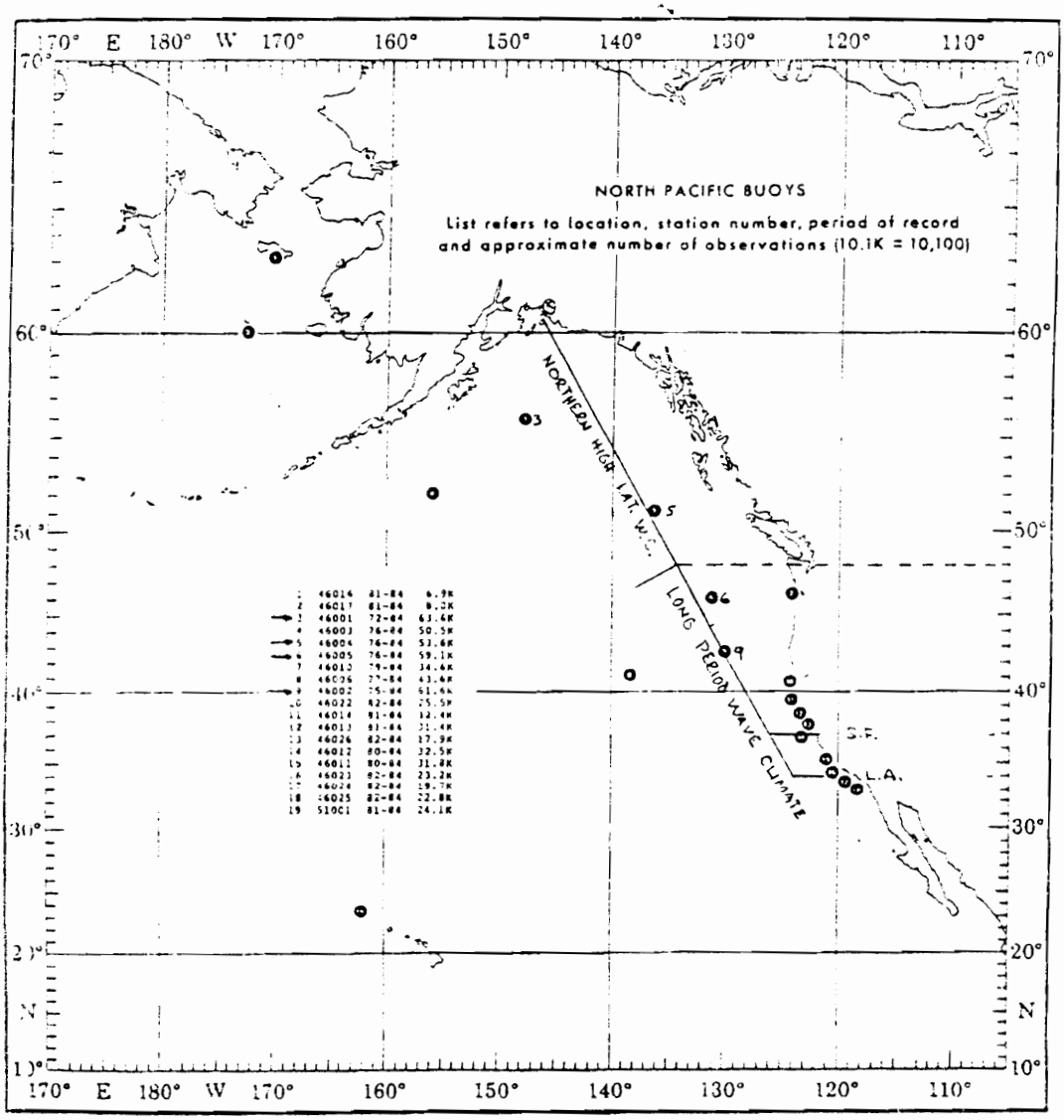

Figure A-1: Relationship of NOAA Buoy Stations 46001, 46002, 46004 and 46005 to TAPS Tanker Route

Table A-1: Percentage Occurrence of Significant Wave Heights at Northern High Latitude Buoy Stations

Hmo (m)	Sta 46001 (%)	Sta 46004 (%)
0-0.5	.61	0.22
0.5-1.5	18.43	18.42
1.5-2.5	32.1	29.21
2.5-3.5	23.84	23.08
3.5-4.5	13.44	14.78
4.5-5.5	6.63	7.92
5.5-6.5	2.74	3.82
6.5-7.5	1.30	1.56
7.5-8.5	0.57	.6
8.5-9.5	0.23	.21
9.5-10.0	0.02	.05
>10.0	0.09	.13

Table A-2: Percentage Occurrence of Significant Wave Heights at West Coast Long Period Buoy Stations

Hmo (m)	Sta 46002 (%)	Sta 46005 (%)
0-0.5	.03	0.14
0.5-1.5	19.05	22.92
1.5-2.5	31.71	30.35
2.5-3.5	23.23	21.59
3.5-4.5	14.55	13.72
4.5-5.5	6.67	6.72
5.5-6.5	2.78	2.67
6.5-7.5	1.13	1.07
7.5-8.5	0.42	0.48
8.5-9.5	0.28	0.27
9.5-10.0	0.07	0.04
>10.0	0.07	0.03

Table A-3: Parameters for the Generalized Wave Spectra for Northern High Latitude Seas.

H_{mo} (m)	k	f_{pr} (Hz)	λ	Amp
1.0	1.00	0.1391	0.616	0.1574
2.0	1.00	0.1160	0.707	0.1883
3.0	1.00	0.0981	0.754	0.2055
4.0	1.00	0.0895	0.784	0.2170
5.0	1.00	0.0834	0.807	0.2261
6.0	1.00	0.0787	0.824	0.2329
7.0	1.00	0.0750	0.840	0.2395
8.0	1.00	0.0719	0.853	0.2449
9.0	1.00	0.0692	0.862	0.2488
10.0	1.00	0.0669	0.868	0.2513
10.9	1.00	0.0652	0.875	0.2543
12.3	1.00	0.0628	0.886	0.2591
13.2	1.00	0.0613	0.891	0.2613

Single Constituent Spectrum:

$$Sw(f) = H_{m_o}^2 \, k \, Amp \left(\frac{f_{pr}}{f}\right)^{4\lambda} \frac{1}{f} \exp\left[-(\lambda + 0.25)\left(\frac{f_{pr}}{f}\right)^4\right]$$

H_{m_0} = Significant wave height

f = Frequency

f_{pr} = Characteristic modal frequency of generalized CWS

λ =Nondimensional shape parameter for Ochi 3P wave spectrum

Table A-4: Parameters for the Generalized Wave Spectra for West Coast Long Period Seas.

H_{mo} (m)	k	f_{pr} (Hz)	λ	Amp
1.0	0.35	0.0840	0.400	0.0949
	0.40	0.1130	1.000	0.3125
	0.25	0.1560	0.850	0.2437
2.0	0.40	0.0800	0.400	0.0949
	0.46	0.0960	0.800	0.2233
	0.14	0.1420	1.300	0.4924
3.0	1.00	0.0843	0.647	0.1676
4.0	1.00	0.0773	0.668	0.1741
5.0	1.00	0.0722	0.682	0.1795
6.0	1.00	0.0684	0.694	0.1837
7.0	1.00	0.0652	0.704	0.1872
8.0	1.00	0.0626	0.712	0.1901
9.0	1.00	0.0604	0.718	0.1922
10.0	1.00	0.0585	0.724	0.1944
11.0	1.00	0.0569	0.738	0.1966
12.5	1.00	0.0547	0.737	0.1992
13.5	1.00	0.0534	0.740	0.2003

Multi-Constituent Spectrum (H_{m_0} = 1.0, 2.0):

$$Sw(f) = H_{m_0}^2 \sum_{n=1}^{3} \left(k\ Amp \left(\frac{f_{pr}}{f} \right)^{4\lambda} \right)_n \frac{1}{f} \exp\left(-(\lambda + 0.25) \left(\frac{f_{pr}}{f} \right)^4_n \right)$$

H_{m_0} = Significant wave height

f = Frequency

f_{pr} = Characteristic modal frequency of generalized CWS

λ =Nondimensional shape parameter for Ochi 3P wave spectrum

k = Weighting factor

Table A-5: Percentage of Occurrence of Seaway Direction at Buoy 46001

	N	NE	E	SE	S	SW	W	NW
Load Ballast	S. Qtr B. Qtr.	P. Bm S. Bm	B. Qtr. S. Qtr	Head Follow	B. Qtr. S. Qtr	S. Bm P. Bm	S. Qtr B. Qtr.	Follow Head
H_{mo}								
0.5-1.5	6.85	8.25	10.80	12.40	15.75	25.65	14.15	7.05
1.5-2.5	7.20	8.10	10.65	11.95	15.05	21.65	16.40	9.00
2.5-3.5	5.45	8.15	13.05	13.15	15.80	21.00	15.35	8.25
3.5-4.5	3.75	8.25	15.10	14.70	15.90	19.80	14.95	7.05
4.5-5.5	4.20	8.10	14.90	17.20	17.90	20.10	11.05	6.35
5.5-6.5	3.55	7.15	16.65	18.25	18.70	18.10	12.50	4.90
6.5-7.5	3.45	8.25	20.25	15.65	13.30	18.90	15.10	5.70
7.5-8.5	1.60	10.50	21.65	16.05	10.50	19.10	16.65	3.65
8.5-9.5	0.00	15.90	24.80	13.90	18.35	23.35	3.00	1.00
9.5-10.	0.00	27.30	4.50	13.50	22.70	31.80	0.00	0.00
>10.0	0.00	7.00	21.00	14.00	7.05	51.15	0.00	0.00

Table A-6: Percentage of Occurrence of Seaway Direction at Buoy 46002

	N	NE	E	SE	S	SW	W	NW
Load Ballast	S. Qtr B. Qtr.	P. Bm S. Bm	B. Qtr. S. Qtr	Head Follow	B. Qtr. S. Qtr	S. Bm P. Bm	S. Qtr B. Qtr.	Follow Head
H_{mo}								
0.5-1.5	19.80	6.50	3.00	5.50	9.85	11.15	16.70	26.90
1.5-2.5	21.35	6.35	3.75	6.15	9.60	11.70	15.40	25.60
2.5-3.5	11.45	4.15	3.95	10.55	16.15	16.55	19.15	18.15
3.5-4.5	4.25	2.85	4.40	12.30	20.35	22.55	20.85	12.55
4.5-5.5	2.35	1.75	3.55	10.05	20.20	23.70	25.55	12.65
5.5-6.5	1.05	0.35	1.55	9.25	23.00	29.10	27.05	8.75
6.5-7.5	0.50	0.10	0.70	9.90	20.50	34.60	22.35	11.05
7.5-8.5	1.85	0.75	1.30	7.70	26.95	33.95	19.30	8.50
8.5-9.5	1.20	1.20	0.80	5.60	20.25	40.85	23.50	6.80
9.5-10.	0.00	0.00	0.00	0.00	26.65	46.65	8.35	18.35
>10.0	0.00	0.00	0.00	0.00	9.10	27.30	48.45	15.15

Table A-7: Percentage of Occurrence of Seaway Direction at Buoy 46004

	N	NE	E	SE	S	SW	W	NW
Load Ballast	S. Qtr B. Qtr.	P. Bm S. Bm	B. Qtr. S. Qtr	Head Follow	B. Qtr. S. Qtr	S. Bm P. Bm	S. Qtr B. Qtr.	Follow Head
H_{mo}								
0.5-1.5	6.55	5.35	6.60	10.70	15.60	15.20	21.50	19.20
1.5-2.5	6.65	4.55	6.15	13.55	16.75	17.65	19.30	16.30
2.5-3.5	5.40	3.30	7.00	15.10	19.35	20.95	17.40	12.40
3.5-4.5	2.90	4.00	8.55	16.15	19.15	24.65	16.45	9.35
4.5-5.5	2.15	3.95	9.75	15.65	20.45	24.45	16.70	8.80
5.5-6.5	1.50	3.00	8.65	19.25	21.95	23.90	18.70	7.10
6.5-7.5	1.10	1.10	11.05	15.65	22.50	34.00	15.95	3.25
7.5-8.5	0.00	0.50	4.75	17.75	24.75	44.75	5.50	3.50
8.5-9.5	0.00	0.00	0.00	17.70	33.85	40.35	3.25	4.85
9.5-10.	0.00	0.00	0.00	35.70	28.55	28.55	3.55	3.55
>10.0	0.00	0.00	0.00	12.80	28.70	28.70	19.15	10.65

Table A-8: Percentage of Occurrence of Seaway Direction at Buoy 46005

	N	NE	E	SE	S	SW	W	NW
Load Ballast	S. Qtr B. Qtr.	P. Bm S. Bm	B. Qtr. S. Qtr	Head Follow	B. Qtr. S. Qtr	S. Bm P. Bm	S. Qtr B. Qtr.	Follow Head
H_{mo}								
0.5-1.5	8.40	3.60	4.35	8.55	14.85	16.35	21.45	22.95
1.5-2.5	7.85	3.75	3.00	6.80	13.95	15.85	22.90	26.90
2.5-3.5	4.75	3.05	4.15	10.25	18.15	19.95	23.85	17.85
3.5-4.5	1.90	2.00	5.15	11.55	23.15	25.05	23.70	9.90
4.5-5.5	1.75	0.95	4.20	11.00	24.70	26.60	25.40	8.40
5.5-6.5	1.60	0.30	2.50	9.20	20.30	31.10	26.60	9.50
6.5-7.5	0.00	0.00	1.85	13.85	29.10	30.10	23.65	2.85
7.5-8.5	0.30	0.30	0.95	9.85	20.80	43.70	21.80	4.10
8.5-9.5	0.00	0.00	0.50	14.20	20.60	51.90	13.70	2.00
9.5-10.	0.00	0.00	0.00	7.10	24.90	60.60	3.55	3.55
>10.0	0.00	0.00	0.00	0.00	13.30	73.30	3.35	10.05

Appendix B: Structural Analysis

Effective Cross Sections

The shell longitudinals can be modeled, for stress purposes, as a fixed end beam with a built-up cross section. The end fixity is derived from symmetric concerns; the longitudinal is continuos over many short bays. Therefore the slope of the longitudinal at each transverse frame is essentially zero.

The built-up cross section, Figure B-1, is composed of three elements: the effective plate flange, the web and the asymmetric flange. The effective plate flange, b_e, is reduced from the full spacing of longitudinals, b, due to shear lag effects[1]. The effective width of the asymmetric flange, b_{fe}, must also be reduced from the full width, b_f. Lehmann has derived a formula for the effective width of an asymmetric flange that is based on an elastic foundation approach[2]. The Atigun Pass tankers have a typical spacing between transverse frames of 202" and a typical spacing between longitudinals of 35".

The effective plate breadth is dependent on the ratio of length between zero moments, L_0, and the spacing of longitudinals, b. For a fixed end beam L_0 is simply half the clear span.

$$L_o = 0.5L = 101" \quad \Rightarrow \quad \frac{L_o}{b} = \frac{101}{35} = 2.9$$

For a beam with a uniform lateral load, the corresponding ratio of effective to full width is,

$$\frac{b_e}{b} = 0.83 \quad \Rightarrow \quad b_e = 0.83b = 29.0"$$

Lehmann's effective width of an asymmetric flange is dependent on a function of αl where

$$\alpha L = \frac{L}{b_f}\left(\frac{1-\nu^2}{6}\left(\frac{t_f}{b_f}\right)\left[\frac{b}{t_f}\left(\frac{h_s}{t_f}\right)^2 + 7.28\left(\frac{h_s}{t_f}\right)^3\right]\right)^{-1/4}$$

and

$$f(\alpha L) = \frac{6}{(\alpha L)^2}\left(\frac{\sinh(\alpha L) - \sin(\alpha L)}{\sinh(\alpha L) + \sin(\alpha L)}\right)$$

$$b_{fe} = \frac{b_f}{2}\left(\frac{1}{1 + 3f(\alpha L)}\right)$$

---

[1]Hughes, O.F., *Ship Structural Design, A Rationally-Based, Computer-Aided, Optimization Approach*, SNAME, Jersey City, NJ, 1988.

[2]Lehmann, E.I., "Practical Applications in Ship Structures". unpublished manuscript, Technische Universitat Hamburg-Harburg, Hamburg, Germany, 1992.

The results of the effective cross section calculation are given in Table B-1. The section properties calculated from the effective cross section are given in Table B-2.

Natural Frequency Analysis

To confirm that the frequency of wave excitation is substantially above the natural frequency of the stiffened panels, and that a static stress analysis is valid, a frequency estimate was made based on the equivalent cross section of the shell longitudinals. The fundamental natural frequency of a fixed end beam in Hz is

$$f_n = 3.57\sqrt{\left(\frac{EI}{\rho L^4}\right)}$$

where: E is the modulus of elasticity

ρ is the mass density per unit length of the beam

Table B-3 contains the result of the frequency analysis.

Stress Analysis

The natural frequency of the stiffened panel is well above the frequency of the wave excitations. A static stress analysis is therefore used and conventional beam equations are valid.

Table B-1: Original and Effective Section Dimensions

Member	b	b_f	h_s	b_e	b_{ef}	αL
	(in)	(in)	(in)	(in)	(in)	
L42	35.0	4.96	15.88	29.0	2.52	4.41
L30	35.0	6.96	21.88	29.0	2.17	2.70
BL	35.0	7.12	26.5	29.0	7.12	

Table B-2: Effective Section Properties

Member	I_{vv}	S_f	S_n	Area
	(in^4)	(in^3)	(in^3)	(in^2)
L42	998.6	66.78	283.2	30.56
L30	1974	101.8	388.4	33.74
BL	5370	288.0	560.3	43.17

Table B-3: Estimated Natural Frequency of Stiffeners

Member	ρ	f_n
	($lb\text{-}s^2/in^2$)	(Hz)
L42	2.24E-02	100
L30	2.48E-02	134
BL	3.17E-02	196

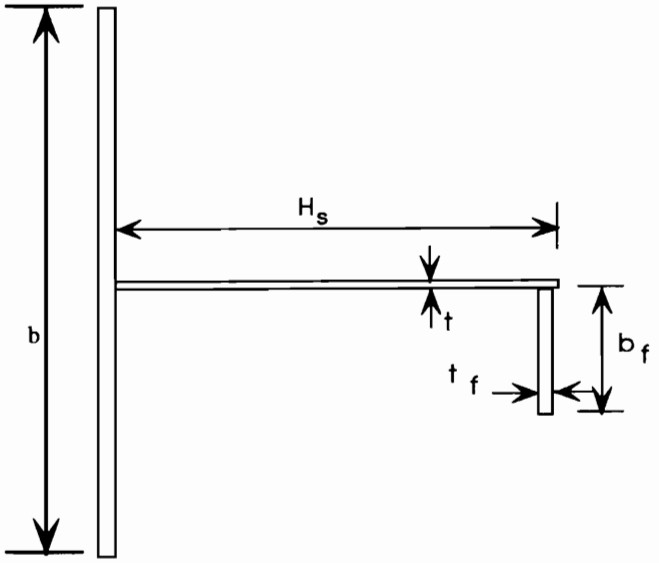

Figure B-1: The Actual Cross Section (Typical)

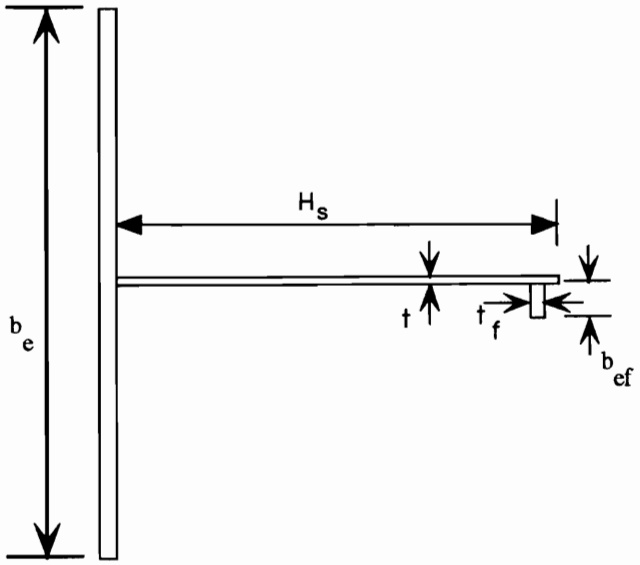

Figure B-2: Effective Cross Section (Typical)

Vita

Paul Franklin was born on April 5, 1964 in Hartford Connecticut and was raised in the suburbs of Boston, Massachusetts. In 1986 he graduated from the University of Alaska-Fairbanks with a Bachelor of Science degree in Civil Engineering and in 1990 from the Johns Hopkins University with a Master of Science degree in Engineering. Before attending Virginia Tech, Paul spent two years as a Noise, Shock and Vibration Engineer in the Hull Engineering Department of Bath Iron Works, Bath, Maine.